GM 65324

2007 FIXED WING MULTISENSOR AIRBORNE SURVEY, ELDOR CARBONATITE AREA

Documents complémentaires

Additional Files

Licence

License

Énergie et Ressources naturelles
Québec

2007 Fixed Wing Multisensor Airborne Survey
(Magnetic, Gamma Ray Spectrometric, VLF-EM)

Eldor Carbonatite Area, Northern Quebec, Canada

NTS 24 C/15,16 and F/1,2 (parts of)

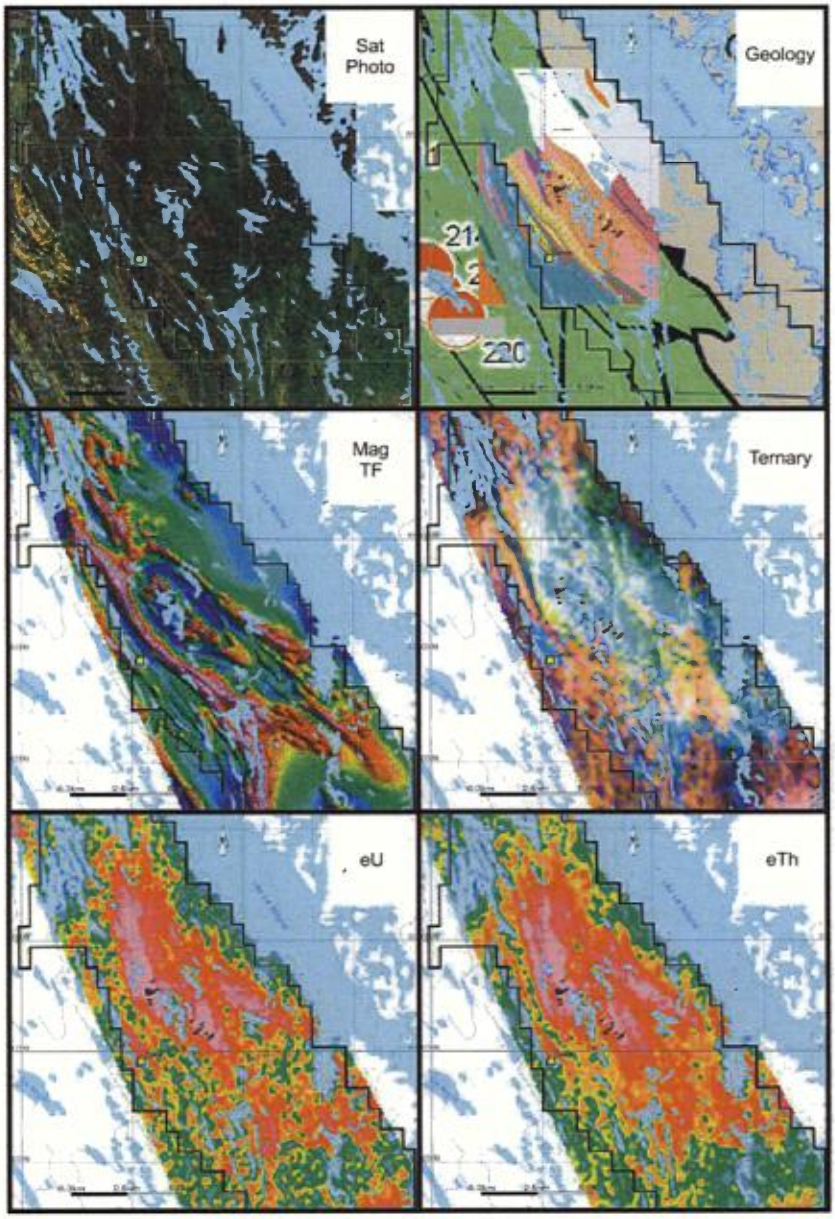

An interpretation report for
Commerce Resources Corp., Vancouver, Canada

R. B. K. Shives, P. Geo.
Ottawa, April 2010

GamX

Gamma Ray Spectrometry for Exploration

Table of Contents

Figures

Tables

Interpretation of Fixed Wing Multisensor Airborne Survey (Magnetic, Gamma Ray Spectrometric, VLF-EM) Eldor Carbonatite Property, Quebec, Canada

1.0 Summary

A fixed wing multisensor airborne geophysical survey was flown in September 2007 by Tundra Airborne Surveys Ltd (Tundra) under contract to Commerce Resources Corp (Commerce), over the Eldor Carbonatite property located in the Nunavik Region of Northern Quebec, Canada. Final delivery by Tundra included digital data and 1:20,000 maps depicting magnetic total field, calculated vertical gradient, total radioactivity (NADR), concentrations of potassium, equivalent uranium, equivalent thorium, and VLF-EM total field. No spectrometric ratios or measured magnetic gradient maps or grids were provided.

Subsequent re-processing of the survey was completed in 2008 by Abitibi Geophysics Inc. (Abitibi), Val D'Or, Quebec, to provide magnetic gradient data, additional grids/maps not provided by Tundra and an interpretation based on more rigorous analyses.

In March, 2009, the author was contacted by Dahrouge Geological Consulting Ltd. (Dahrouge) to conduct additional interpretation, with emphasis on delineation of possible radioactive element zoning within the carbonatite phases and detection of new occurrences.

To support interpretation of the airborne survey, the author assembled a georeferenced database incorporating all airborne layers with information provided by Dahrouge (geochemical results from rock and soil sampling, bedrock geology, diamond drilling, known occurrence locations) and the previous interpretations by Abitibi. The latter focused primarily on magnetic and VLF-EM interpretation with less emphasis on the radiometric information.

Aeromagnetic patterns accurately map the distribution of magnetic minerals (mainly magnetite) within the carbonatites and enclosing host rocks. The known showings are related to discrete magnetic highs in two areas (NW and SE Zones) but additional known zones of interest (Ashram, Star Trench and Eastern) lie in magnetically low zones areas. Two lower priority, interpreted new anomalies occur in high-magnetic areas to the south. Drilling to date may be biased towards the magnetic highs. Strong magnetic contrasts throughout the survey define sharp, open folds with offsets and breaks providing constraints to lithologic and structural interpretation.

Airborne gamma ray spectrometric patterns reflect only moderate lithologic variation within the host rocks based on the presence of felsic units in dominantly mafic rocks. In contrast, discrete anomalies over known carbonatite showings reflect some combination of in-situ bedrock and glacially modified (dispersed) material. All spectrometric layers are required for proper interpretation, but eU, eTh and related ratios with K appear most effective.

The airborne survey provides valuable exploration guidance. An initial, somewhat cursory examination of the airborne survey data was conducted by the author in 2009 and provided to Dahrouge as a draft PDF format report in December. Some of the questions raised in the draft report have been addressed in this final version. Remaining questions can be addressed with further study of existing information and new data generated during 2010. Recommendations include incorporation of all currently available data to further improve the interpretation of the airborne data and define additional, location-specific exploration targets. Creation of an improved Ternary map had been recommended, has now been completed and is included in this report. Magnetic susceptibility measurements on all cores and outcrops are recommended. Rigorous examination of the detailed stacked profile data offers drill targeting assistance. Ground follow-up to selected targets (coordinates are provided) should include ground radiometric reconnaissance (scint/spectrometry) to guide prospecting, sampling and preliminary evaluation. Subsequent, systematic surveying, soil sampling and trenching should be conducted where warranted.

2.0 Introduction

Airborne surveys provide a means for remotely sensing geophysical and geochemical properties of geological materials located on or below the earth's surface. Most commonly, these surveys measure magnetic, electromagnetic and radioactive characteristics of bedrock and overburden cover. Where these properties vary in response to bedrock geology, alteration or potentially economic mineralization, the surveys can provide mineral exploration guidance.

Worldwide, carbonatites are commonly enriched in a variety of rare earth elements (REEs) and many other metals, including radioactive elements uranium and thorium. Although the latter elements may not occur in economic concentrations their natural radioactivity provides useful pathfinders to the host intrusions and specific phases within them. Canadian examples include deposits located in Oka (Quebec), Cantley (Quebec), Allen Lake (Ontario) and many others. Recent study by the author at the Blue River carbonatites in British Columbia have shown airborne and in-situ gamma ray spectrometry can be used to detect, delineate and separate Nb-rich phases from Ta-rich phases based on their relative enrichments in Th and U.

Both sovitic and beforsitic phases of carbonatite have been identified at the Eldor Carbonatite. Mineralization grading up to 11.4% Nb2O5 and 0.21% Ta2O5 has been discovered in several zones.

To support new exploration on the Eldor Property, Commerce completed a fixed wing magnetic /gamma ray spectrometric/VLF-EM survey in 2007, under contract with Tundra Airborne Surveys Ltd.

The author received the airborne data and additional geological information from Dahrouge Geological Consulting Ltd. in June 2009. This report describes the airborne survey and its interpretation, focusing on the radiometric data with reference to magnetic data where appropriate, incorporating information provided by Dahrouge. Emphasis has been placed on relationships of the airborne geophysical patterns to the regional and local bedrock geology, drill core geochemistry, the carbonatite and its various phases, and mineralization currently defined. Recommendations are provided.

Acknowledgment

While working on this interpretation project, the author experienced several personal events which delayed completion by months. The author sincerely thanks Commerce Resources Corp. and Dahrouge Geological Consulting Ltd. for their patience. Darren Smith of DGCL is especially thanked for this and for providing information and data requested in a timely manner.

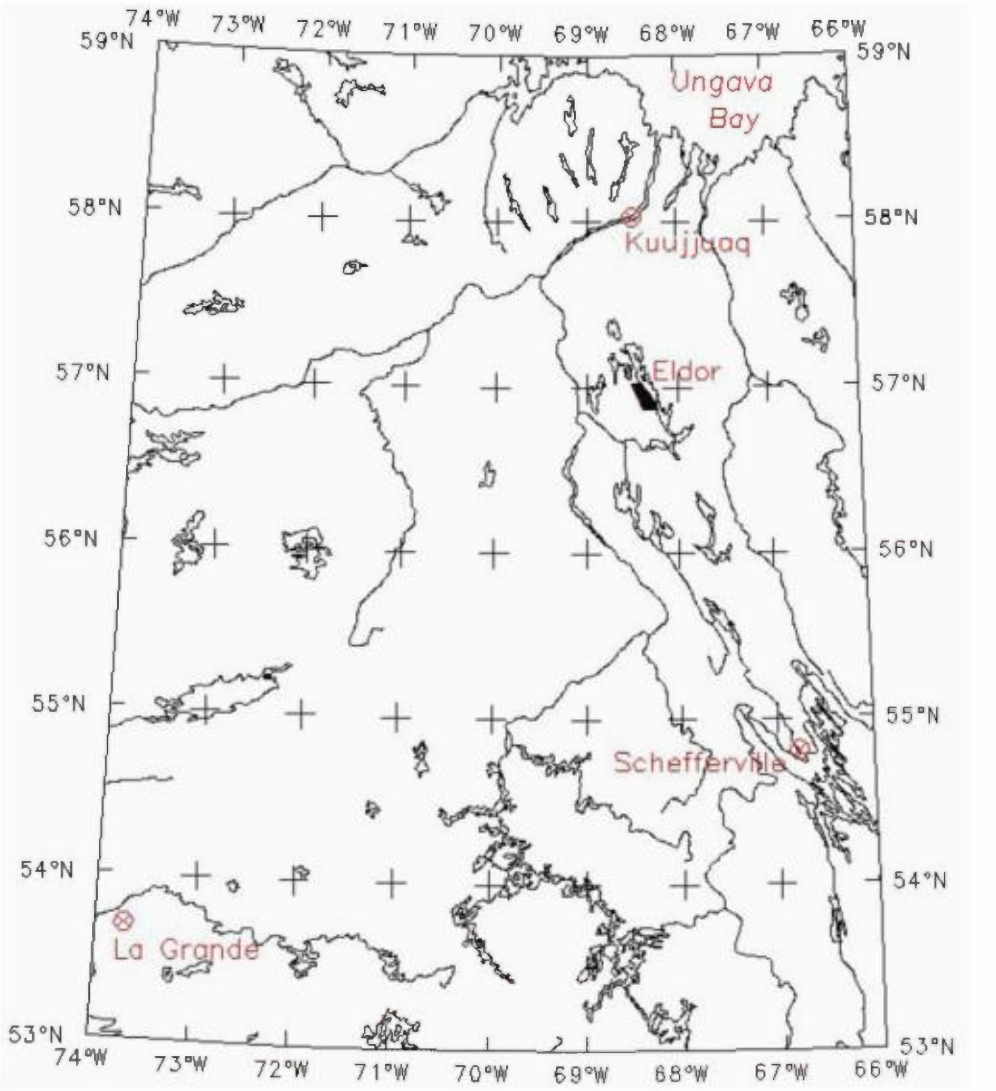

Figure 1. *Airborne survey location (small black polygon) and base of operations in Kujjuuaq, Nunavut. Image courtesy Tundra Airborne Surveys.*

3.0 Summary of Property Geology

To support discussion of the airborne results, regional and local bedrock geology has been summarized below from Geologie Quebec publication MM2005-01 entitled "*Lithotectonic and Metallogenic Synthesis of the New Quebec Orogen (Labrador Trough)*, by Thomas Clark and Robert Wares, provided to the author by Dahrouge in PDF format.

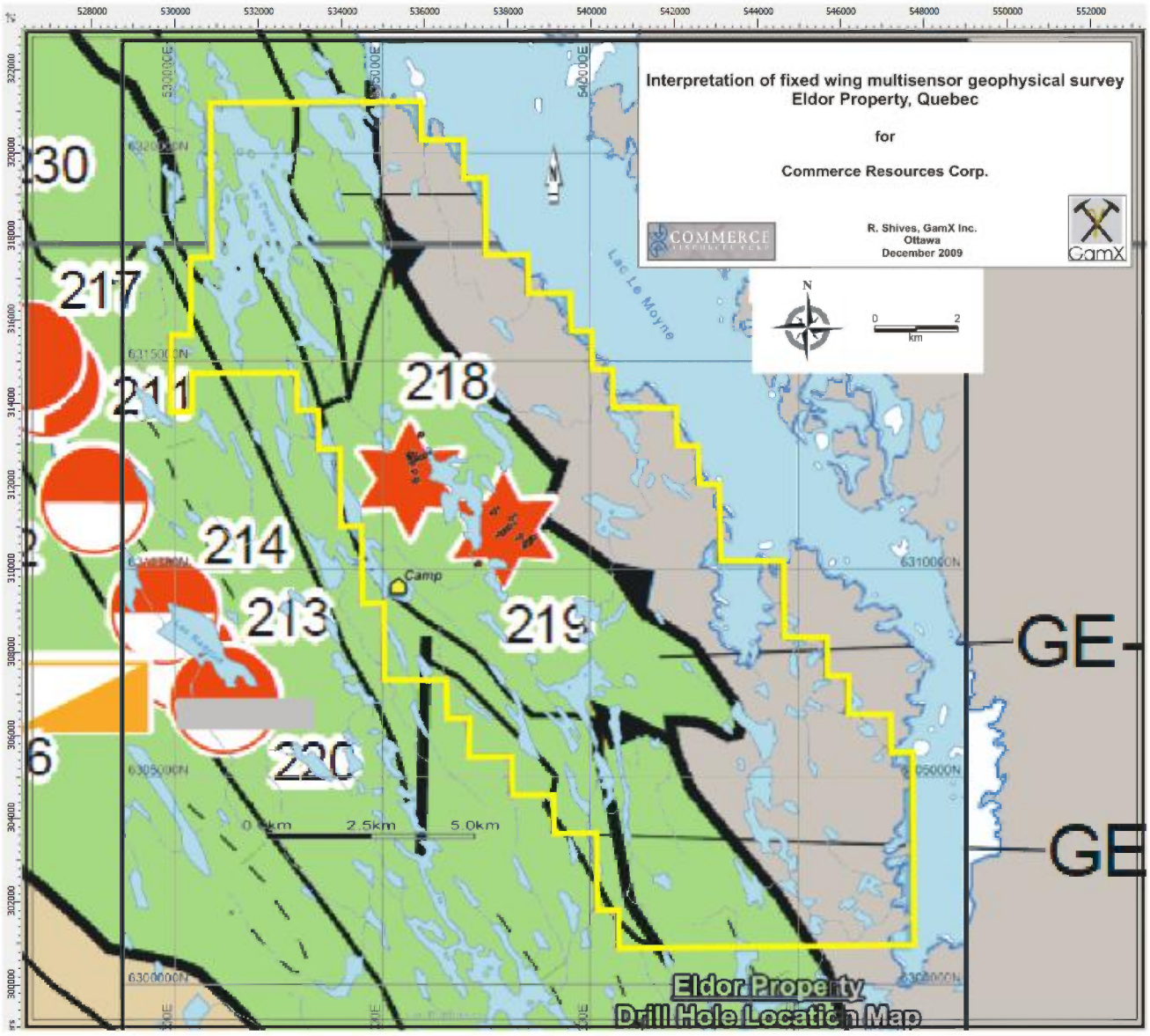

Figure 2. *Regional geology (from report MM2005-01) with Commerce Eldor Property boundary (yellow), lakes, areas of diamond drilling.*

The property is elongated in a NW direction, parallel to the gross regional geological strike. A major, folded, regional thrust fault called the Herodier Fault separates the property along its axis into an eastern lithotect (SC Zone) containing Proterozoic paraschist, paragneiss and amphibolites, and a western, allochthonous part (Gerido Zone) containing the LeMoyne and Doublet Groups, intruded by the Eldor Carbonatite (Figure 2).

The Doublet Group rocks (basalts, iron formation, and pyroclastites) lie below and are older than the Le Moyne Group rocks. The Le Moyne Group is composed of felsic volcanic (rhyodacite) and sedimentary (dolomite, shale, pelites) rocks of the Douay Formation, overlain by platformal rocks of the Aulneau Formation (conglomerate, dolomite, dolomitic tuff). The Aulneau sequence includes mafic and ultramafic tuffs contemporaneous with the Eldor Carbonatite, which has been mapped as a subvolcanic intrusion into the Le Moyne Group only.

According to Clarke and Wares (2005) the base of the Doublet Group contains mafic pyroclastic rocks (amygdaloidal tuffs, agglomerate, breccia), basalt flows, graphitic shales, pyritic shale, quartzite, greywacke and massive pyrite beds, all assigned to the Murdoch Formation. These originated from a series of explosive mafic volcanic cones or fissures (so have little lateral stratigraphic continuity) and were deposited into shallow, reducing waters.

The Eldor carbonatite (Figure 3) is considered Paleoproterozoic in age, based on dating of a rhyodacite within the host Le Moyne Group, at 1870+/-3 Ma. The rocks have undergone greenschist facies metamorphism. As mapped, the complex is approximately 15 km long by 4 km wide. It contains both intrusive and extrusive equivalents of massive, brecciated and ultramafic carbonatite, and marginal tuffs interpreted as a possible volcanic apron.

3.1 Mineralization

Clark and Wares state that mineralized rocks within the Eldor Carbonatite contain bastnasite [$(La,Ce)CO_3F$], columbite [$(Fe,Mn,Mg)Nb_2O_6$], pyrochlore [$(Ca,Na)_2Nb_2O_6(OH,F)$], monazite [$(La,Ce,Nd)PO_4$] and fluorite, producing anomalous concentrations of Nb, Ta, La, Ce, P, U and Th. Biotite-pyrochlore-rich phases (glimmerite) appear as marginal phases.

Exploration to date has produced four named mineralized zones, designated Northwest, Southeast, Ashram and Star Trench zones (Figure 4). A fifth unnamed area has recently been indicated to the east of the mapped complex, where carbonatite outcrop has been discovered.

Results from drilling conducted in 2008 by Commerce suggests there are several primary magmatic phases of carbonatite (pers. comm. D. Smith, DGCL, Oct, 2009):

> "*The first phase is mineralogically simple (accessory minerals phlogopite-magnetite) and is generally not well mineralized. It intrudes, fragments and strongly alters the metavolcanic(?) wall rocks to aggregates of phlogopite and carbonate.*
>
> *The second phase hosts most of the Nb-Ta mineralization discovered to date, and is composed of coarse-grained beforsite containing megacrystic magnetite, abundant apatite and accessory aegirine, melilite and other exotic silicate phases. Mineral banding is variably developed. Nb and Ta appear to be present principally in columbite in the Northwest mineralized area and in pyrochlore in the Southwest area.*
>
> *The third phase of carbonatite intrusion dominates the Southeast and Strar Trench areas. It is finer-grained, apparently lower temperature and more volatile-rich, as it brecciates and often strongly alters the earlier carbonatite phases it intrudes. This phase is generally mineralogically simple and accessory mineral poor (phlogopite-pyrite-fluorite-hematite). The presence of hematite suggests it is significantly more oxidized that the first two phases.*
>
> *The fourth phase occurs as very fine grained grey-green REE-rich dykes (10 cm to 2 m thick) that crosscut all rocks, and is found in boulders and outcrop in the Ashram Peninsula area.*
>
> *The zones appear to have different mineralogies, with fluorite common in the Southeast, Star Trench and Ashram areas but less abundant in the Northwest Area, where magnetite is abundant. Niobium appears more abundant in the Northwest Area. Tantalum is more abundant in the South East and Star Trench areas."*

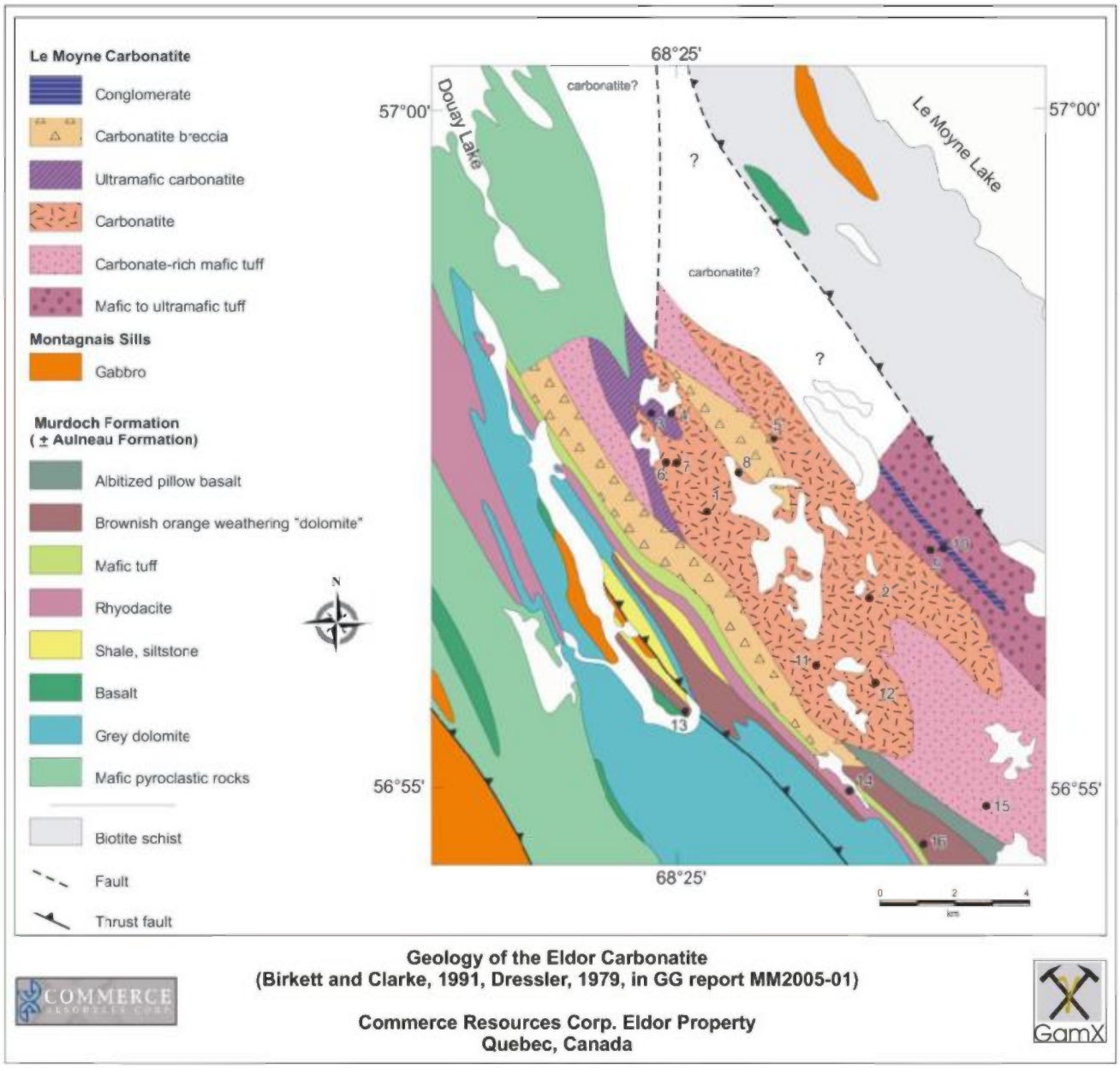

Figure 3. *Geological sketch map of the Eldor carbonatite (Also termed Le Moyne carbonatite). Numbered sites refer to mineral deposits in SIGEOM database and samples collected during reconnaissance sampling conducted by Birkett and Clark (GG Report MM2005-01)*

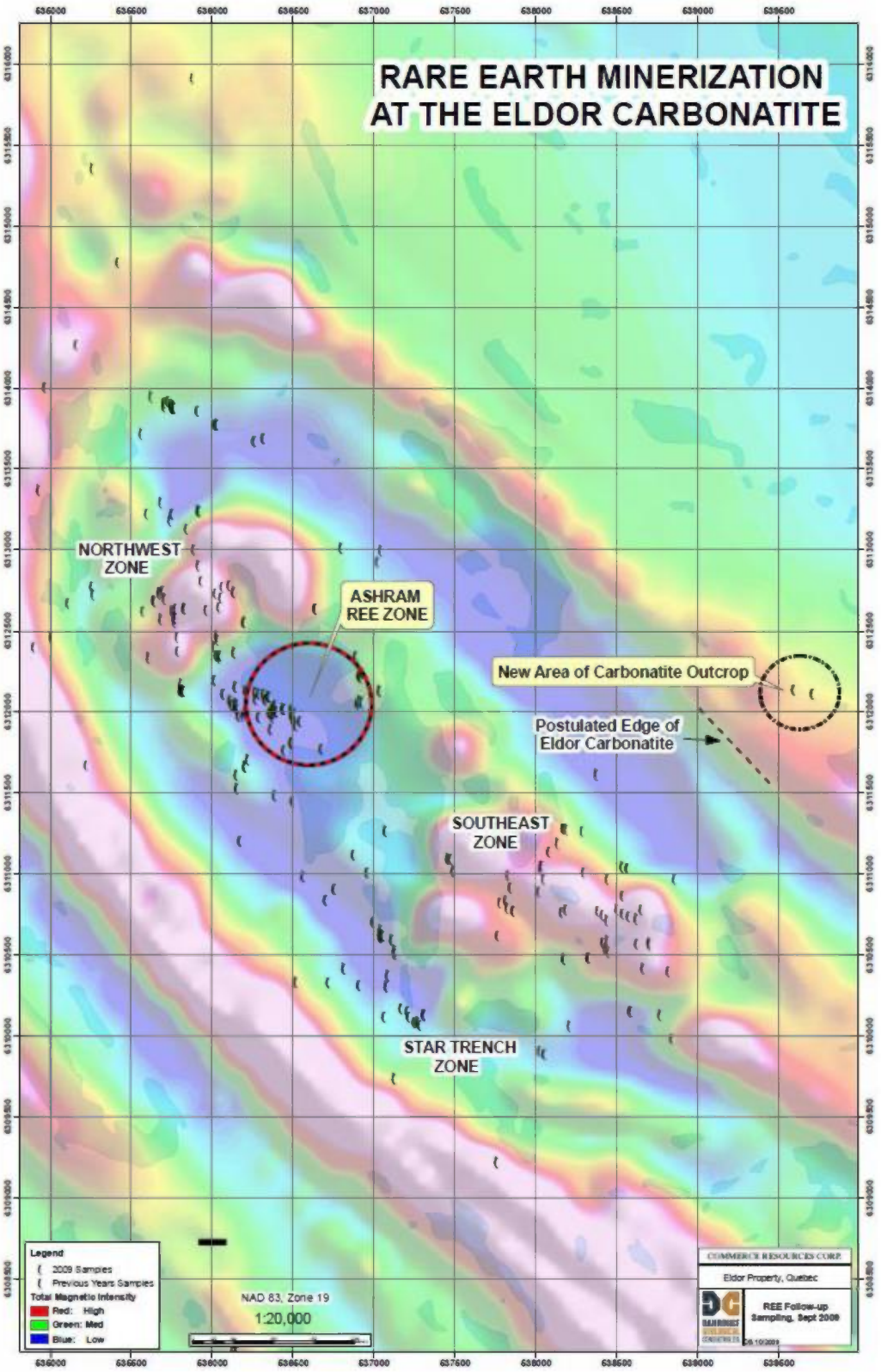

Figure 4. *Location of existing Zones within the Eldor Carbonatite area, overlain on aeromagnetic patterns. Image supplied by D. Smith, (DGCL).*

3.2 Drill Core Assay data

The author has compared analyses of roughly 3000 drill core samples, comparing Ta and Nb values with K and U and Th values from the geochemical analyses (not determined radiometrically).

The following series of graphs illustrate the results. The first three images compare U, Th and K with Ta2O5, respectively. The second set of three images compare U, Th and K with Nb2O5, respectively.

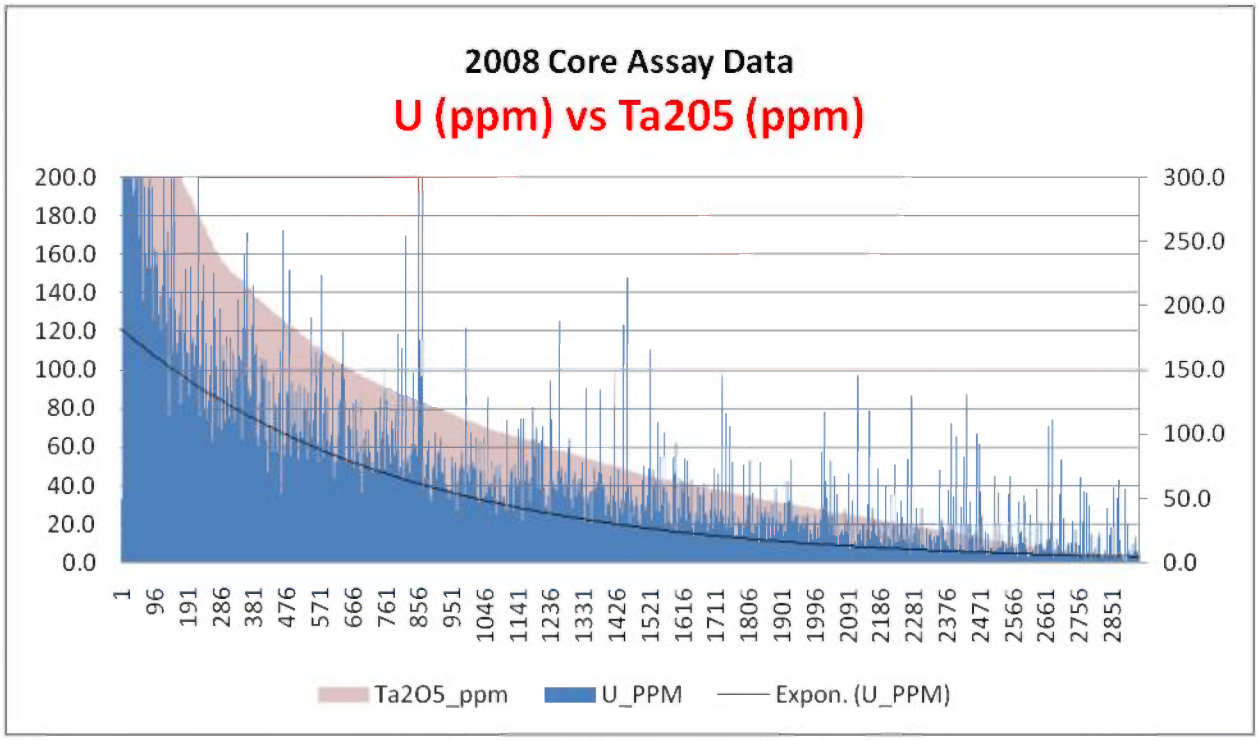

Figure 5. *Drill core assay data: U vs Ta_2O_5*

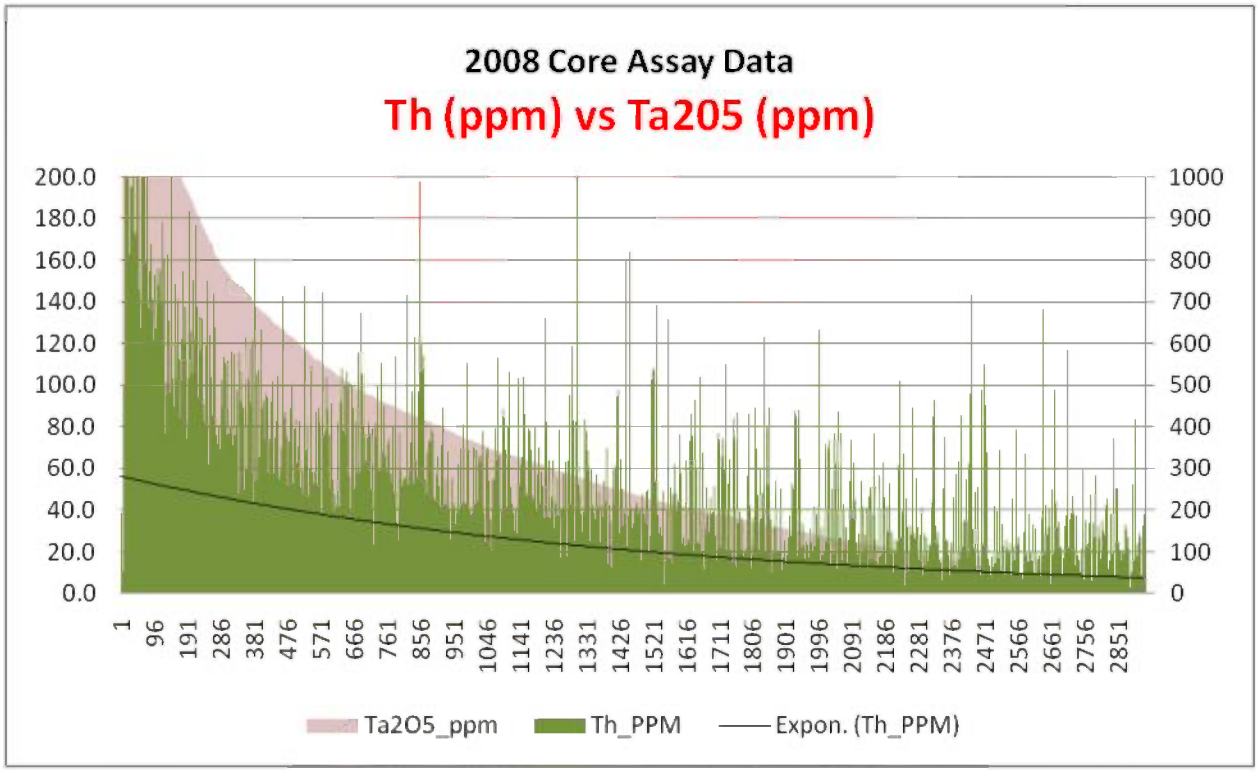

Figure 6. *Drill core assay data: Th vs Ta_2O_5*

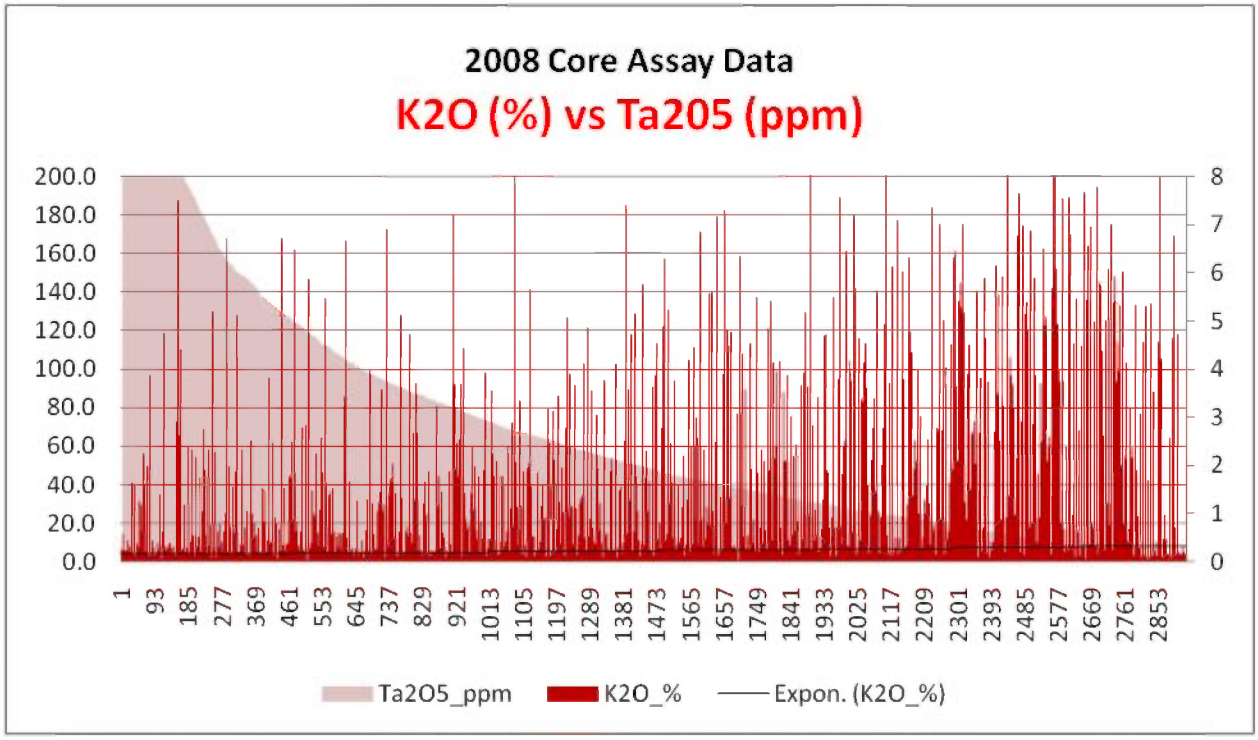

Figure 7. *Drill core assay data: K_2O vs Ta_2O_5*

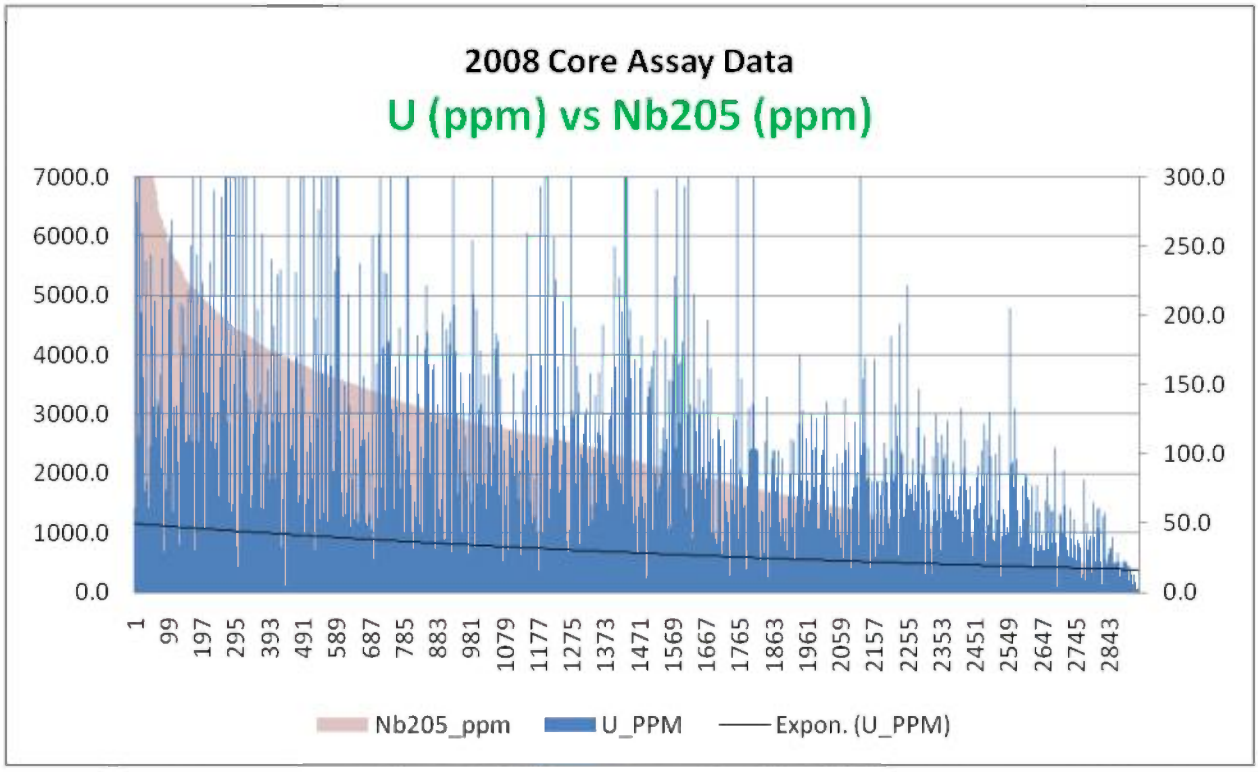

Figure 8. *Drill core assay data: U vs Nb_2O_5*

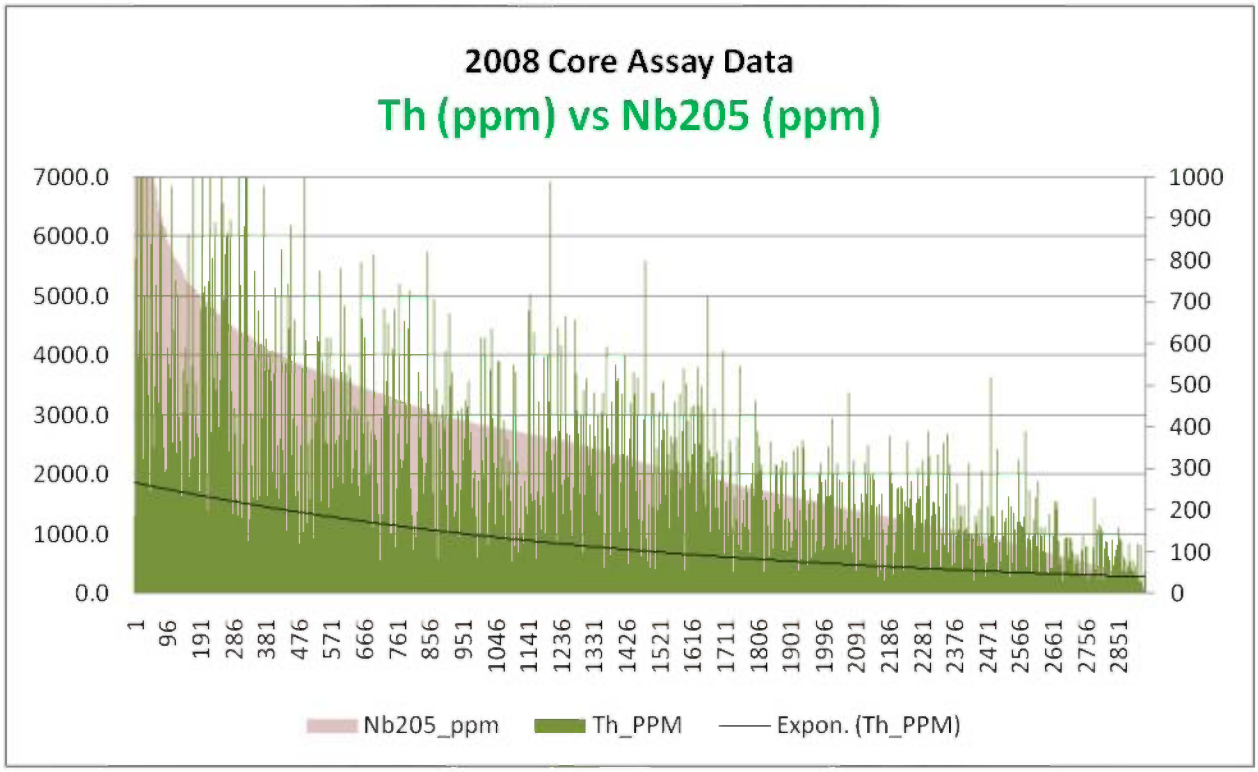

Figure 9. *Drill core assay data: Th vs Nb_2O_5*

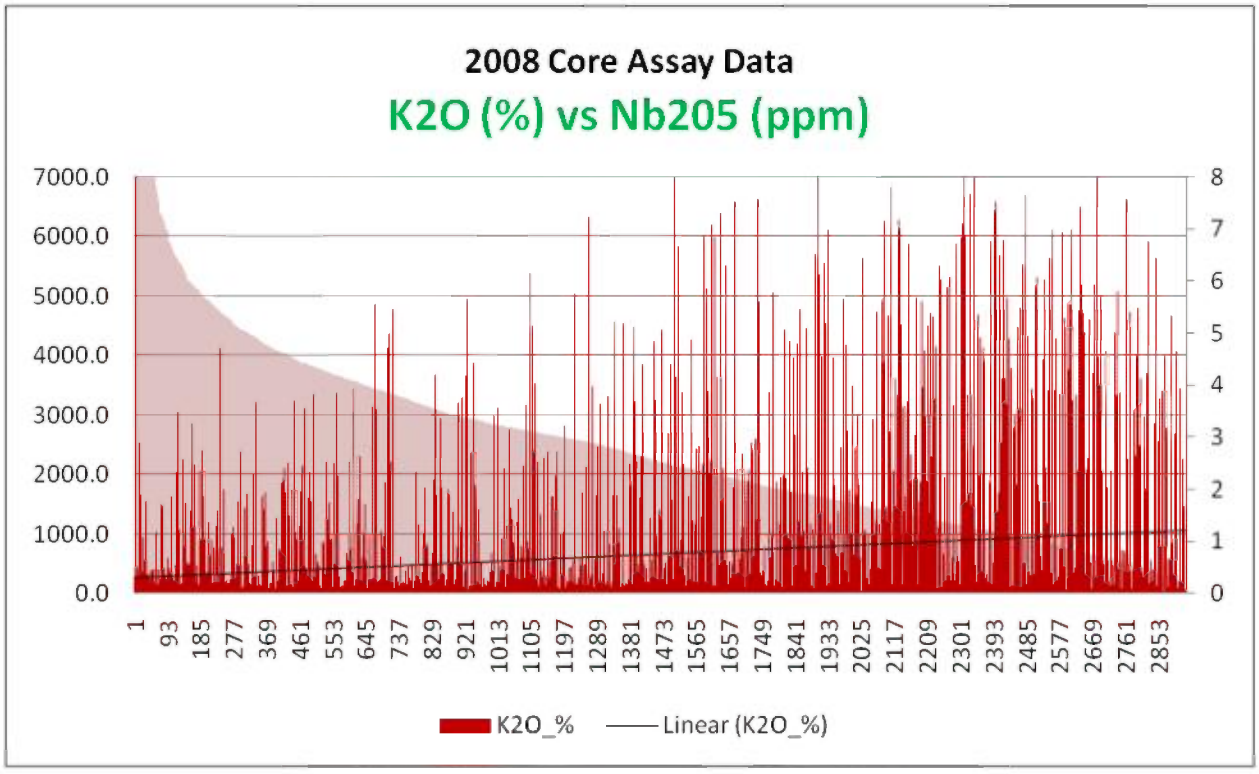

Figure 10. *Drill core assay data: K_2O vs Nb_2O_5*

In the above figures, the degree of correlation is indicated by the shape of the "best fit" line (black line) with the Ta or Nb oxide concentration distribution curves (shown as solid violet shape in background of each graph). Clearly, Nb is best correlated with Th, Ta with U and neither Nb nor Ta with K. These relationships support the airborne radioactive element interpretation presented.

To further illustrate relationships between U, Th, Nb, and Ta, the author conducted a more rigorous comparison of ALL drill core elements analysed, using Microsoft Excel 2007's "correlation analysis tools". The data included 2931 analyses of 61 elements (a total of 193,511 values). The resulting correlation matrix supports recognition of inter-relationships between all elements. The matrix has been provided digitally as a separate PDF file. The large size of the PDF image cannot be easily depicted in the current report document, so only a portion of the image is shown below.

The Excel worksheet function calculates the correlation coefficient between two measurement variables when measurements on each variable are observed for each of N subjects. (Any missing observation for any subject causes that subject to be ignored in the analysis). The correlation analysis tool is particularly useful when there are more than two measurement variables for each of N subjects. It provides an output table (the correlation matrix). The correlation coefficient is a measure of the extent to which two measurement variables "vary together", scaled so that its value

is independent of the units in which the two measurement variables are expressed. The value of any correlation coefficient must be between -1 and +1 inclusive.

	SiO2_%	Al2O3_	Fe2O3_	MgO_%	CaO_%	Na2O_	K2O_%	TiO2_%	P2O5_	MnO_%	Cr2O3_	Ni_PPM	Sc_PPM	Ba_PPM	Be_PPM	Co_PPM	Cs_PPM	Ga_PPM	Hf_PPM	Nb_PPM	Ta_PPM	Th_PPM	U_PPM	U/Th
SiO2_%	1.00																							
Al2O3_%	0.94	1.00																						
Fe2O3_%	0.17	0.14	1.00																					
MgO_%	0.22	0.26	0.28	1.00																				
CaO_%	-0.64	-0.66	-0.53	-0.83	1.00																			
Na2O_%	0.66	0.72	0.13	0.07	-0.44	1.00																		
K2O_%	0.88	0.91	0.12	0.31	-0.63	0.41	1.00																	
TiO2_%	0.40	0.43	0.44	0.16	-0.44	0.33	0.38	1.00																
P2O5_%	-0.23	-0.24	0.19	0.09	-0.03	-0.14	-0.23	0.13	1.00															
MnO_%	-0.13	-0.14	0.37	0.55	-0.41	-0.08	-0.14	0.08	0.03	1.00														
Cr2O3_%	0.35	0.34	0.08	0.11	-0.25	0.24	0.34	0.13	-0.11	-0.02	1.00													
Ni_PPM	0.25	0.25	0.16	0.09	-0.22	0.17	0.23	0.26	-0.04	0.01	0.77	1.00												
Sc_PPM	0.22	0.20	0.50	0.23	-0.39	0.24	0.13	0.23	0.25	0.23	0.12	0.09	1.00											
Ba_PPM	0.43	0.43	-0.07	-0.21	-0.04	0.32	0.40	0.09	-0.20	-0.27	0.14	0.07	0.01	1.00										
Be_PPM	0.10	0.11	0.02	0.08	-0.10	0.20	0.05	0.01	0.07	0.01	0.02	0.02	0.03	0.39	1.00									
Co_PPM	0.35	0.37	0.55	0.26	-0.50	0.31	0.32	0.69	0.30	0.14	0.20	0.36	0.34	0.04	0.04	1.00								
Cs_PPM	0.84	0.85	0.13	0.26	-0.56	0.41	0.93	0.35	-0.27	-0.15	0.32	0.21	0.13	0.43	0.01	0.30	1.00							
Ga_PPM	0.86	0.88	0.36	0.28	-0.68	0.60	0.84	0.50	-0.09	-0.02	0.29	0.24	0.32	0.39	0.11	0.46	0.80	1.00						
Hf_PPM	0.02	0.00	0.33	0.17	-0.21	0.05	-0.01	0.13	0.29	0.08	-0.02	0.00	0.35	-0.08	0.00	0.23	-0.03	0.16	1.00					
Nb_PPM	-0.18	-0.18	0.17	0.04	0.02	-0.14	-0.16	0.05	0.41	0.05	-0.08	-0.03	0.22	-0.08	0.12	0.13	-0.17	-0.11	0.19	1.00				
Ta_PPM	-0.12	-0.15	0.23	-0.05	0.02	-0.08	-0.14	0.02	0.46	0.02	-0.06	-0.05	0.40	-0.08	-0.01	0.13	-0.15	0.01	0.35	0.25	1.00			
Th_PPM	-0.21	-0.22	0.07	-0.11	0.15	-0.14	-0.23	-0.05	0.39	-0.02	-0.09	-0.08	0.50	-0.06	0.00	0.00	-0.22	-0.16	0.21	0.46	0.54	1.00		
U_PPM	-0.11	-0.13	0.19	0.02	-0.03	-0.05	-0.13	0.03	0.52	0.04	-0.06	-0.05	0.37	-0.10	-0.02	0.15	-0.14	0.02	0.41	0.23	0.88	0.48	1.00	
U/Th	0.04	0.00	0.19	0.03	-0.09	0.04	0.01	0.02	0.24	0.03	0.00	-0.01	0.03	-0.04	-0.01	0.15	0.01	0.16	0.32	-0.07	0.45	-0.18	0.53	1.00
Rb_PPM	0.85	0.85	0.11	0.27	-0.57	0.34	0.96	0.34	-0.25	-0.15	0.32	0.23	0.07	0.41	0.03	0.28	0.94	0.81	-0.04	-0.16	-0.15	-0.24	-0.15	0.02
Sn_PPM	0.00	-0.03	0.53	0.06	-0.18	-0.02	-0.03	0.39	0.36	0.13	-0.01	0.08	0.61	-0.05	0.00	0.47	-0.06	0.13	0.32	0.43	0.41	0.43	0.32	0.08
Sr_PPM	-0.29	-0.33	-0.41	-0.86	0.82	-0.22	-0.30	-0.30	-0.18	-0.47	-0.13	-0.14	-0.30	0.22	-0.15	-0.39	-0.24	-0.36	-0.22	-0.08	-0.01	0.08	-0.06	-0.06
V_PPM	0.05	0.05	0.61	0.24	-0.35	0.05	0.04	0.69	0.29	0.29	0.07	0.25	0.24	-0.15	0.03	0.59	0.00	0.16	0.14	0.24	0.11	0.04	0.13	0.03
W_PPM	-0.01	-0.01	0.00	0.05	-0.03	0.00	-0.01	0.03	0.00	0.02	0.00	0.16	0.01	-0.02	0.00	0.02	-0.01	-0.01	0.01	0.00	0.00	0.00	0.01	-0.01
Zr_PPM	-0.03	-0.05	0.32	0.15	-0.17	0.01	-0.07	0.11	0.33	0.10	-0.04	-0.01	0.30	-0.10	0.01	0.20	-0.08	0.11	0.98	0.24	0.34	0.23	0.39	0.30
Y_PPM	-0.33	-0.30	-0.05	0.13	0.05	-0.17	-0.31	-0.04	0.52	0.21	-0.13	-0.09	0.09	-0.22	0.08	0.02	-0.35	-0.24	0.17	0.19	0.15	0.29	0.21	-0.04

Table 1. *Drill core assay data: Correlation Matrix (only reproduced in part here)*

Note that in the matrix, the author has colour coded values according to negative (blue) or positive (red) hues. The intensity of the hue indicates degree of correlation. Thus, deep red colours indicate strongly positive correlation (ie. Rb and Cs are positively correlated with K20) and deep blue colours indicate strongly negative correlation (ie. CaO and Sr versus MgO). Yellow hues indicate low positive correlation.

Although this approach has been conducted without regard for host lithology, important geochemical patterns can be discerned, and the author recommends Dahrouge continue to search for useful geochemical correlations/pathfinders. Relationships between Nb, Ta, U and Th can now be semi-quantified based on the drill core assays:

Ta vs U = 0.88
Ta vs Th = 0.54

Nb vs Th = 0.46
Nb vs U = 0.23

As a function of this relationship (Ta better correlated with U, and Nb better correlated with Th), the U/Th ratio provides a strong discriminator, as shown in the Table above (positive correlation of U/Th ratio with Ta (0.45) and low negative correlation with Nb (-0.07). The author suggests that a similar approach could be taken for carbonatitic samples only (exclude the non-carbonatite samples) in order to improve discrimination. However, as stated above, the existing relationships support the airborne radioactive element interpretation presented.

4.0 Airborne Geophysical Survey

The survey was flown September 26, 2007 by Tundra Airborne Surveys Ltd., using a Beechcraft King Air 65A90 (registration N41J) owned and operated by Dynamic Aviation Group, Virginia. Magnetic measurements were recorded at 10 per second from three sensors: two were mounted 16.3 m apart in wing-tip pods and the third was 10.4 m rearward in a tail stinger. A Pico-Envirotech GRS410 spectrometer collected 256 channel gamma ray spectra every 1 second from 33.6 litres of downward-looking NaI detectors and a single 4 litre upward-looking crystal. A Hertz Totem 2A VLF receiver was used to measure secondary electromagnetic fields produced as a response of near-surface conductive materials to primary electromagnetic fields generated by remote transmitters used for submarine communications (stations NLK Jim Creek, Washington and NAA Cutler, Maine).

Figure 11. *Beechcraft King Air used to conduct the Eldor Property survey in 2007. Magnetic sensors were carried in wing-tip pods and tail-mounted stinger. Spectrometer detectors (33.6 litres) were carried on board. Photo courtesy Tundra Airborne Surveys Ltd.*

Ancillary equipment provided realtime GPS and video tracking, radar and barometric altimetry, and an SDAD-1 data logger. Additional details about the airborne system, calibrations, specifications, tests, data collection, processing and presentation are provided in the survey report provided to Commerce by Tundra in pdf format.

Flight lines were east-west oriented, spaced at 200 m intervals, with north-south oriented control lines every 2000 m (Figure 5). Terrain clearance was nominally 60m. Aircraft speed was nominally 136 knots, or approximately 70 meters per second.

Final data were presented to Commerce digitally in GeoSoft .gdb and ascii formats, and as maps of total magnetic field, calculated magnetic vertical gradient, K, eU, eTh, NADR and VLF total field contours, all with flight paths and topographic base. No data interpretation was provided in the Tundra Logistics Report which accompanied the data.

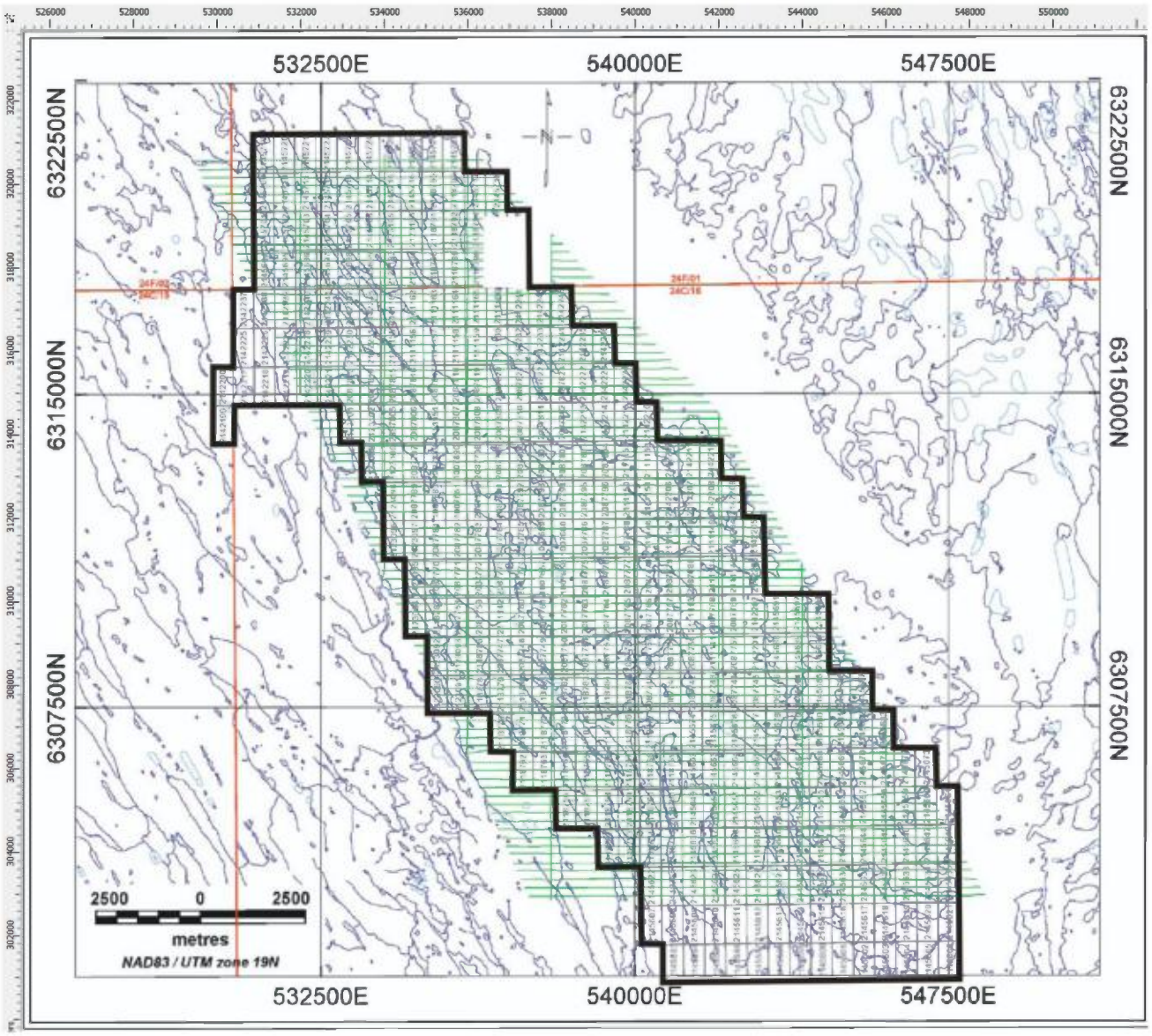

Figure 12. *Survey layout showing 200m east-west oriented flight lines with 2000m north-south oriented control lines (green) overlain on claim map, property boundnary. Image courtesy Abitibi Geophysics Inc.*

5.0 Airborne Survey Interpretation

To support interpretation of the airborne survey a geographically registered, multi-layered database was created by the author using CorelDraw X4, incorporating georeferenced images of airborne gridded layers, as supplied by Tundra and Abitibi and generated by the author using GeoSoft's Oasis Montaj. These were combined with regional geological information (GG Report MM2005-01) and local information provided by D. Smith, DGCL.

Map views of the airborne data (Appendix 1) are derived by gridding data collected along each flight line, to interpolate values for grid cells lying between the 200 m flight lines. While necessary to create useful maps, this inherently smoothes the data along and between the flight lines. To view the data with maximum resolution it is best to use the original flight line data for each parameter. Stacking several parameters on a single flight line profile provides a means to view all data layers on a single profile, to better display interrelationships. This was done by the author using GeoSoft Oasis Montaj to display K, eU and eTh profiles for selected line segments.

Unfortunately, the different sampling rates for magnetic and VLF data (sampled 10 times per second) and the spectrometric data (sampled 1 time per second) makes it difficult to fuse the two datasets into a single database. This can be done if the magnetic data is resampled to 1 Hz (with loss of some information) but for this survey the magnetic data were provided by Tundra as a separate GeoSoft database, preventing inclusion of the magnetic data on the spectrometric profiles.

The Digital Terrain Model (DTM) for the area offers significant mapping aid, as it depicts ridges and valleys which mimic stratigraphic variation within the belt. It should be used (judiciously) to constrain geological strike, and is referred to below.

5.1 Aeromagnetic Data

Several well defined magnetic features occur within the Eldor carbonatite and enclosing host rocks, as mapped. In many areas, narrow, curvilinear magnetic highs coalesce and diverge (defining canoe-shaped anomalies), reflecting moderately open folding, synformal and antiformal structures. Terminations indicate fold noses (ends of the canoes) in several areas, and sharp offsets or kinks suggest late brittle faulting. Clearly, many of the curvilinear trends reflect magnetic strata (flows, tuffs or coarser pyroclastic deposits) or stratiform intrusive sills within the host rocks to the carbonatite intrusion. It is not clear to the author which features may reflect primary lithologic variation during build-up of the volcano-sedimentary sequence, versus secondary features related to possible pre- and syn-folding intrusion of magnetic sills, related to subsequent magmatic activity (carbonatitic or otherwise). Incorporation of site-specific information provided by surface bedrock/drill core geology and measurements of magnetic susceptibility (outcrop and drill core) will support improved interpretation, and this should be conducted in specific areas of interest. Some of these features are best viewed on the higher frequency data provided on derived magnetic products such as the

analytic signal, first vertical derivative, magnetic tilt (especially) and apparent susceptibility layers. Where these features have spatial or genetic relevance to areas of specific exploration or mapping interest, such as in the vicinity of the existing mineralized zones, it is recommended that Commerce use the interactive "sun-angle" shading approach available in GeoSoft (and other software) to best delineate them. The results can be dramatic, in terms of fault delineation. This was not performed by the author during this study. Abitibi used this method but they presented only results based on either a southwest or northeast illumination source, which accentuates NW-SE strata-parallel features, difficult to separate from lithological strike. An interactive approach will highlight magnetic breaks in all directions.

The magnetic patterns associated with the Eldor carbonatite form a NNW-elongated "snow-shoe" shaped pattern. Within the carbonatite, primary magmatic phases (described above) contain variable magnetite contents, and this is reflected in the magnetic patterns. The Northwest and Southeast Zones (as indicated on material supplied by Dahrouge) contain high-magnetic phase(s) which are not radiometrically distinguishable (as exposed on surface) as they both contain relatively lower K, higher eTh and eU (see Zone descriptions below for more detail). In contrast, Ashram and Star Trench Zones, and many other occurrences (numbered 3, 4, 5, 6, 7, 9, 10, 11, 12 on Figure 3) lie within moderate to deep magnetic lows. The magnetic patterns within the carbonatite reflect folding which mimics the external patterns, suggesting internal folding of sill-like phases, post-intrusion/extrusion. If this is correct, then future exploration should consider "strike" of the phases.
Does mineralization within occurrences 3,4,5,6,7,9,10,11,12 and Star Trench have a common relationship to a peripheral low-magnetic carbonatite suite, and those at Northwest and Southeast Zones relate to a centralized, high-magnetic suite? Does Ashram relate mineralogically more to the former, given its low magnetic signature?

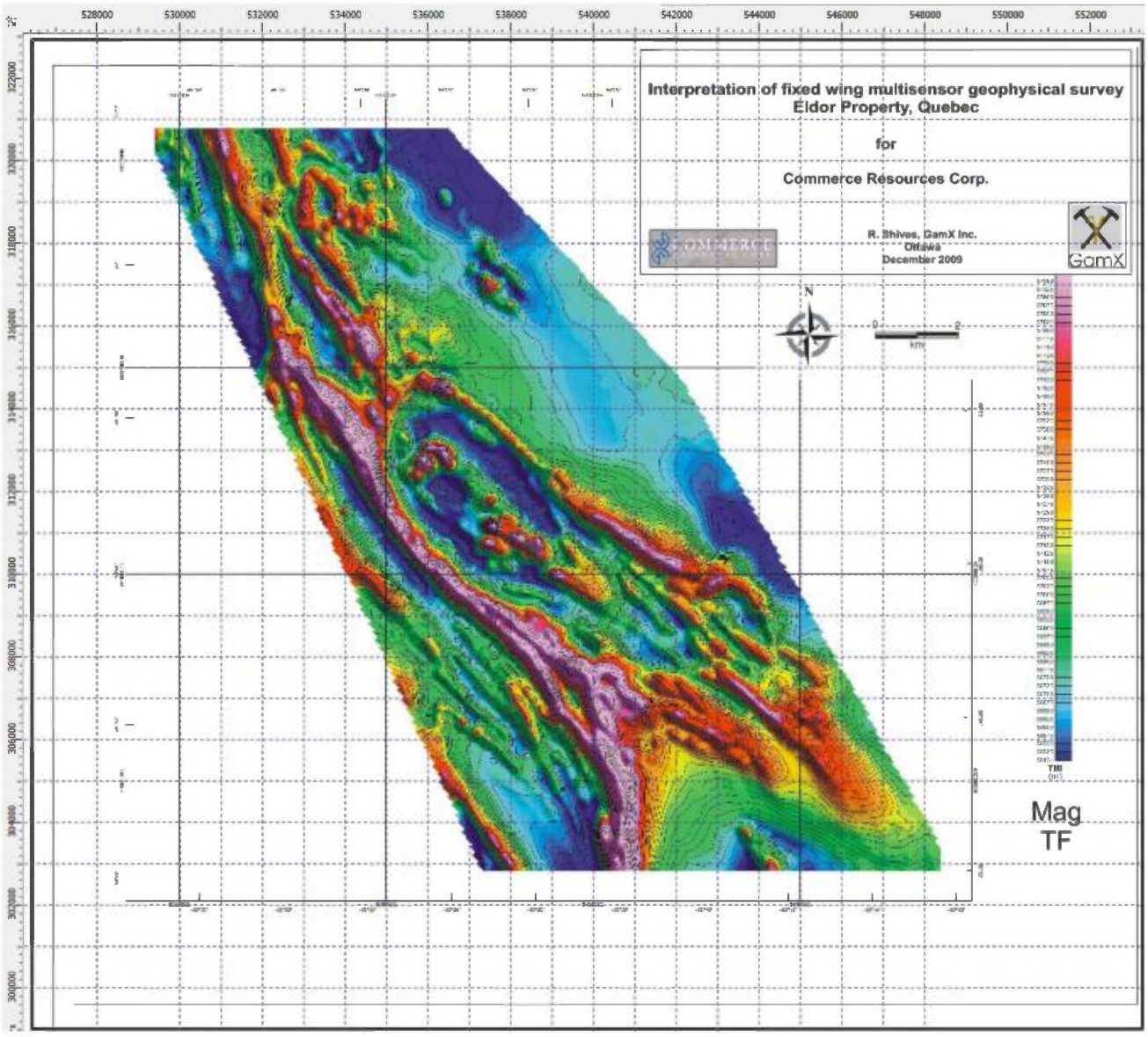

Figure 13. *Magnetic Total Field map*

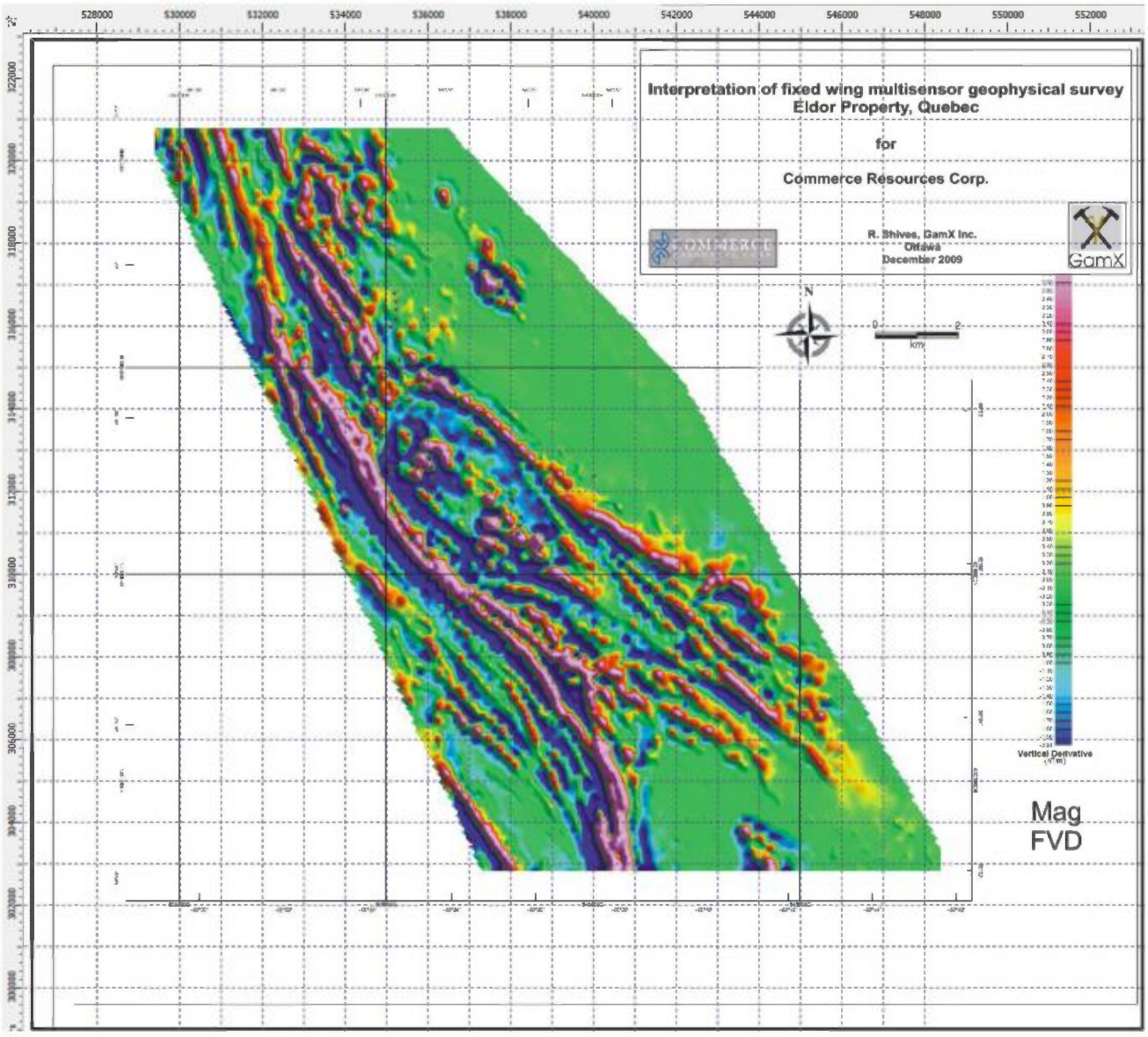

Figure 14. *Magnetic first vertical derivative map*

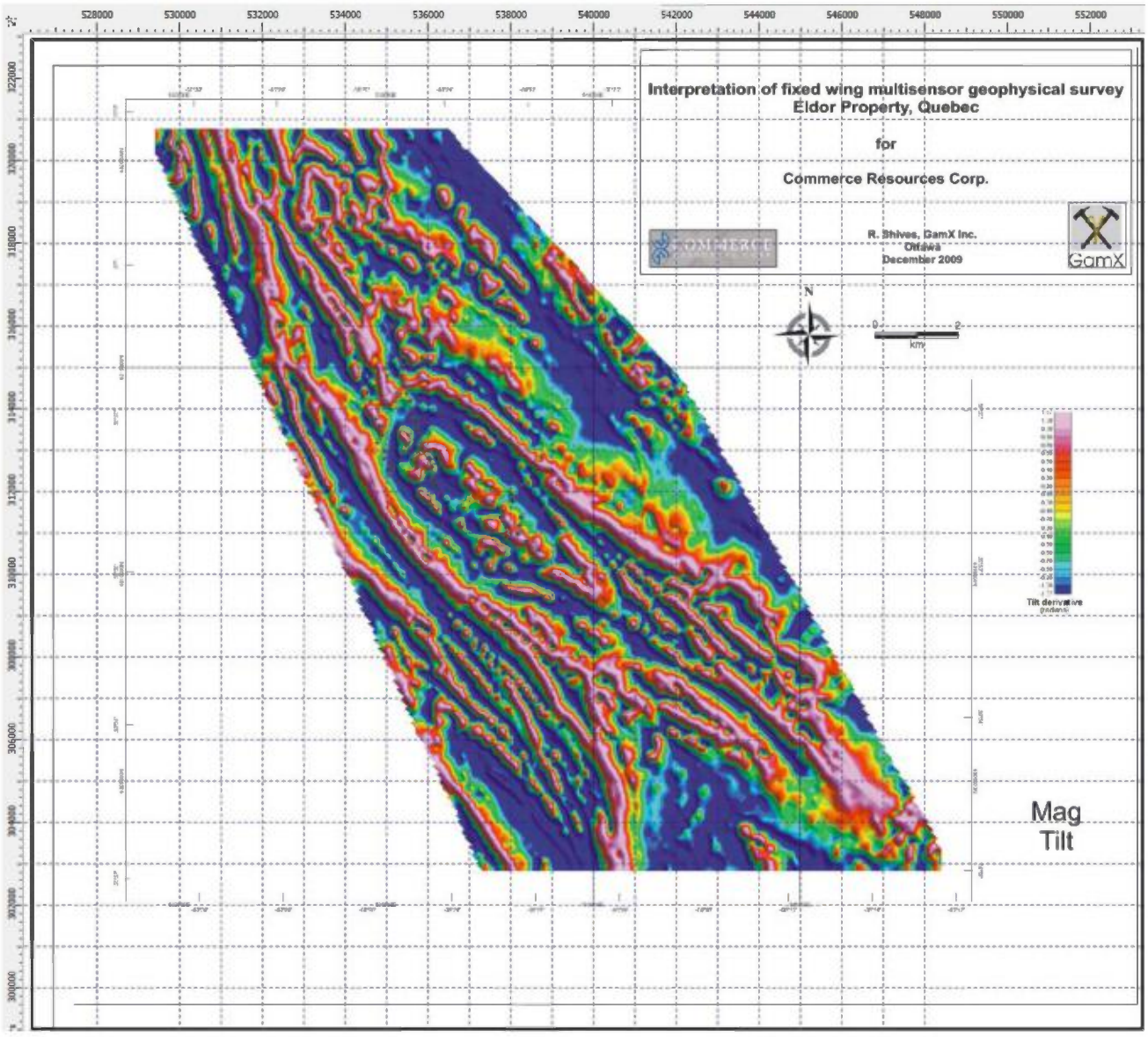

Figure 15. *Magnetic tilt map*

5.2 Airborne Gamma Ray Spectrometric Data

Full interpretation of the gamma ray spectrometric data requires examination of all layers provided by Tundra in both map and stacked profile form, combined with all other available geological layers. The airborne spectrometric technique provides estimates of the concentrations of K, U and Th determined using gamma ray radioactivity which emanates naturally from the top 30 cm of the earth's surface. Unlike magnetic and electromagnetic (potential field) measurements, there is no significant depth penetration. Radiometric responses are directly affected by soil and surface moisture variations such that swampy, low ground, lakes, snow or ice attenuate the signal, resulting in lowered responses in all three measured radioactive elements. To reduce or eliminate effects due to topographic variations, soil moisture and several other factors, radioactive element ratios can be used to detect important relative variations between the elements, to aid bedrock mapping and detection of alteration.

The at-surface geochemical (K, U and Th) nature of airborne gamma ray spectrometry means that radioactive element patterns must be interpreted in relation to the geology (bedrock or overburden) on the surface. For this reason, correlation with conventional bedrock and soil geochemistry can be more direct than the deeper-sensing magnetic/electromagnetic methods, which require rock property information to constrain interpretation. Increased bedrock exposure due to thin or no overburden, and areas with little or no vegetation, may cause an increase in the measured total radioactivity and the values for all three radioactive elements. This exposure effect can be seen on both map and profile views of the data and must be considered during interpretation. A similar, generally less intense effect occurs over forest clear-cuts, where the removal of trees and related reduction in soil moisture tends to increase the overall measured radioactivity, but none are anticipated in the Eldor property area. Again, the use of ratios can minimize these effects, allowing detection of subtle relative enrichment or depletion of one or more radioactive elements.

Radiometric data collected over water (lakes and large rivers) represents background radioactivity with very low counts rates, indicated by deep blue "low" colours on the corresponding radioactivity maps. Note that in these areas the radioactive element ratios are unreliable due to very low, statistically invalid count rates. These may produce high amplitude, false anomalies on the ratio maps. Conventionally, these effects are minimized by related gridding techniques and by masking the gridded data with drainage ("water-mask" overlay).

As the spectrometric method estimates U and Th concentrations based on measurements of daughter isotopes (Bi-214 and Tl-208, respectively) assumed to be in equilibrium with their parent isotopes (Bi-214 and Th-232, respectively) we refer to the concentrations as "equivalent", symbolized as "eU" and "eTh". This universal convention is followed in the Tundra products and in this report.

Dahrouge has reported that glacial transport direction is from the south towards the north, throughout the survey area. This has important implications for the application of the airborne spectrometric patterns to related ground followup. The linear nature of the eU and eTh trends suggests there may be a significant down-ice dispersion influence, and this must be considered. Ground follow-up should target the up-ice portions of these trends, at least initially, and then work along the trend in a down-ice direction (northerly in this case) if results warrant continued work.

The following Sections describe radioactive element patterns in relation to geological bedrock and known occurrences based on information provided to the author. The distribution of geological units has been derived from the regional mapping (Figure 2) and more local Eldor (Le Moyne) mapping (Figure 3)

5.2.1 Potassium (K) map

Gridded potassium values range from zero to over 2 %K. Patterns are dominated by blue lows over water (<0.25 %K) with irregular or linear highs in several areas. These higher K areas have been numbered K1 to K7 for reference (see K airborne figures, below)

K1 is a NNW trending 1 km wide by 3.5 km long area which spans portions of three mapped units southeast of Lac Douay (Doublet and Le Moyne Groups and the Eldor carbonatite northern phase). More detailed bedrock mapping (Figure 3) shows discordance with the K trend, underlain by mafic pyroclastic rocks of the Murdoch Formation to the north, and mafic tuff, ultramafic carbonatite or carbonatite breccia to the south (labeled as K3, roughly 700 m southwest of the Northwest Zone drilling). **These rock types are typically low in K, suggesting either mis-mapped bedrock geology or the presence of locally exotic glacial cover in the high-K area. The former explanation appears more likely. Comparison with the DTM indicates that topo highs correlate with maximum K values, suggesting a possible bedrock exposure influence, but again, supporting a "non-overburden" K source.**

K2 refers to 4 elongated K highs located along the western border of the survey, along the eastern shore of Fox lake (Commerce's exploration camp). Again, these highs trend somewhat obliquely to the locally mapped bedrock contacts, but in part they overlie rhyodacitic rocks mapped within the Murdoch Formation. As these potassium highs coincide with moderate thorium values (see eTh map) they are interpreted as accurately reflecting the distribution of the rhyodacite, in turn suggesting revision to the mapped geology in that area (both location and strike of the bedrock lithologies). Several other airborne layers support this, including the magnetic first vertical derivative (FVD), which shows a strong linear high trend immediately east of the high K-eTh trend. (The "deeper sensing" nature of magnetic measurements relative to the at-surface, radiometric signal source, suggests the magnetic linears are not reflecting glacial dispersion trends.) The digital terrain model for the area also indicates topographic trends which support a revision to the mapped

geology depicted in Figure 3 (where ridges believed to reflect geological strike trend across mapped contacts).

K3, the southern extension of K1, probably maps the extension of the same (unidentified) bedrock geological unit, lying along moderately lower ground immediately west of the Northwest Zone drilling. Narrowing of the K trend in the vicinity of K3 may be in part due to masking by water in the two small lakes (and adjoining low ground) located west and northwest of the NW Zone. The unit may actually underlie these lakes. If so, then it is possible that the lowermost intersection of the deepest-drilled holes in the NW Zone may have cut this higher-K unit.

K4 lies immediately south of the eastern area of new carbonate outcrops, in an area mapped as mafic to ultramafic carbonatite tuff. Again the mapped bedrock geology does not explain the airborne K values here. Comparison with the magnetic FVD patterns suggests the K-rich unit is magnetic, NW trending, and continues to the south. This is very similar to the K3 anomaly on the west side of the carbonatite. Indeed, the continuity of the magnetic signature around the eastern, northern and western edges of the carbonatite (the wooden frame of the snowshoe) suggests a relationship. Does this represent a fenitic border to the carbonatite? Or is it a K-rich mafic sill intruding the volcanosedimentary sequence pre-carbonatite? The spatial relationship between K4 and the carbonatite outcrop area (with its high eU and eTh signature – see below) presents a structural puzzle, as the carbonatite material occurs east of the K anomaly, and east of known carbonatite as mapped.

K5 and K6 cover a 5 km^2 area (large) south of the detailed mapping area (shown in Figure 3) but still within the regional, mapped contact of the carbonatite. Weak eTh and eU are associated with this area, suggesting the K does not directly overlie carbonatitic material. Note that eU and eTh is anomalous in adjacent areas to the south and southeast (see below).

Although K2 appears related to felsic host rocks west of the mapped extent of the carbonatite, the remaining K anomalies (K1, K3, K4, K5, K6) lie peripherally, close to the carbonatite rocks and not within the carbonatite body proper. The author is not aware of descriptions of fenitization associated with the Eldor (Le Moyne) carbonatite, but the K distribution does suggest this is possible.
Alternatively, it has been stated that biotite-rich pyrochlore (glimmerite) occurrences are located at the margins of the carbonatite. Is it possible that K anomalies in some locations might relate to the biotite within these units? If so, they offer “prime” exploration vectors.

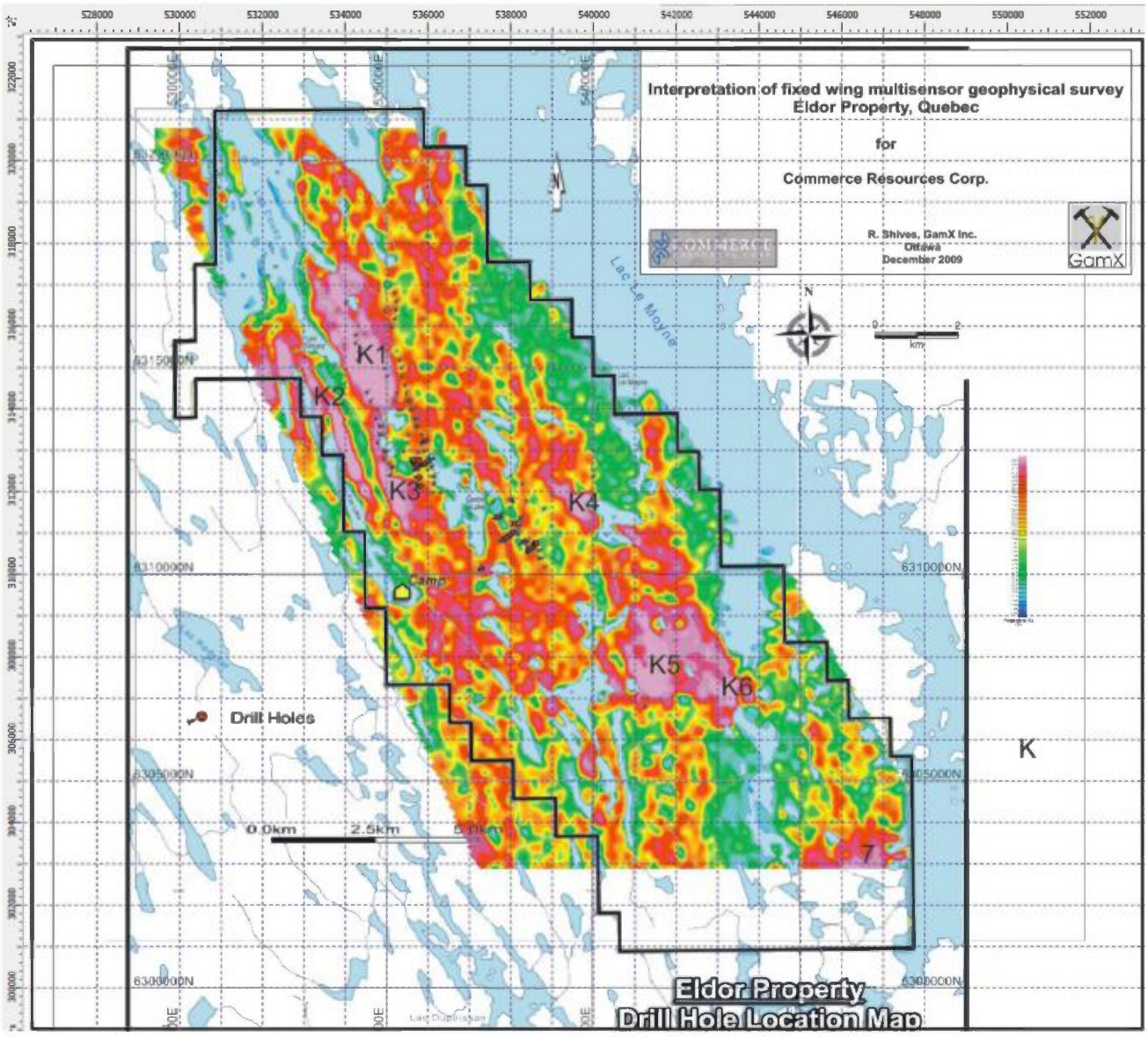

Figure 16. *Airborne Potassium map*

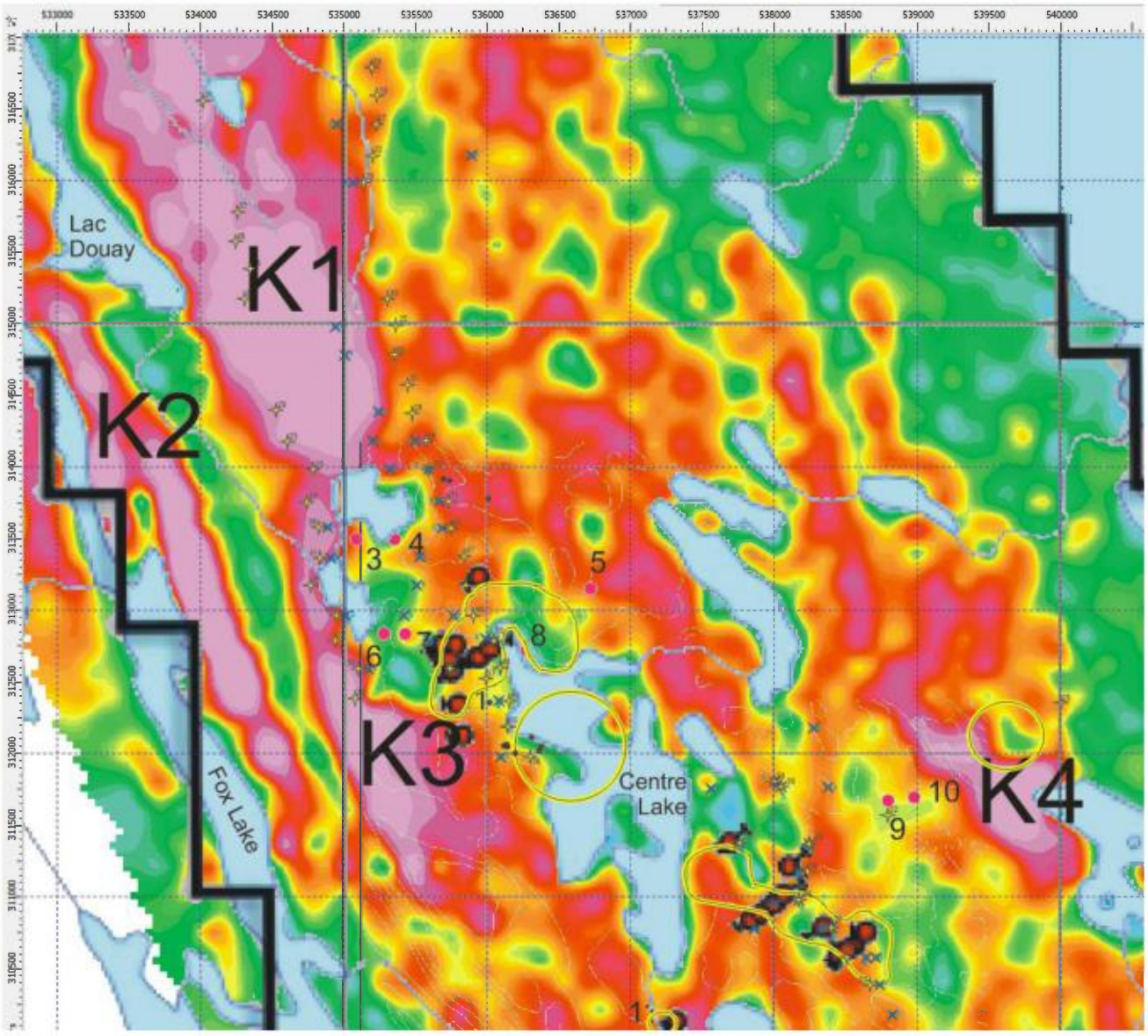

Figure 17. *Airborne Potassium map, zoomed,overlain with specific flight line anomalies picked using GeoSoft from the profile data, where the* ***yellow " + " symbols are eTh maxima, and the blue " x " symbols are eU maxima*** *(symbols also plotted on subsequent images below).*

5.2.2 equivalent Uranium (eU) map

Relative eU highs that are tentatively interpreted as non-carbonatite-related (primarily because of their locations farther from known carbonatite occurrences) include moderate amplitude anomalies in the extreme NW corner of the survey (**eU4**, with no associated K or eTh), and along Fox Lake adjacent to and extending north of the exploration camp (**eU5**, eTh is associated, but very low K). The significance of these anomalies is unknown to the author. Perhaps further examination of these including a brief site visit is warranted.

Within the main carbonatite body and possibly extending beyond the mapped eastern contact, are three large eU anomalies, **eU1, eU2 and eU3**. These patterns each appear to result from subparallel, eU-rich trends, which are best delineated on the higher resolution (less filtered) stacked profile plots (discussed below).

A clear spatial association is apparent between eU highs and the known Northwest (eU1) and Southeast (eU2) zones defined by exiting drilling. There is also a strong uranium anomaly (eU3) associated with the eastern outcrops of carbonatite, lying over that area but extending over a larger, NW-SE trend north of the area.

Correlation of the airborne eU patterns with Ta2O5 results in rocks and soils is outstanding, such that eU offers good approximation of Ta in the near surface materials. Of course, the density of the airborne readings is much higher than the soil sampling, allowing good correlation between the km-spaced soil lines.

The general association of uranium with Ta-enriched phases at several carbonatites, and as demonstrated locally at Eldor based on existing drill core analyses and soil samples (described above) provides strong evidence of the potential utility of the eU patterns to guide exploration. Glacial transport may have significantly extended the airborne response down-ice (reportedly to the north, in the range from 345 degrees to 015 degrees) from their points of origin in the bedrock, and this factor must be considered initially. The parallel nature of the northern extents of eU1, eU2 and the two lobes of eU3, support this concept of glacial dispersion, defining a 345 degree trend. However, the apparent transport distance based on the long axis of the eU patterns is quite different, with eU3 anomalies measuring roughly 1 km long, eU2 roughly 2.5 km and eU1 roughly 6 km long. This suggests that there is anomalous source bedrock lying along the eU1 trend rather than a single point source, perhaps presenting an improved exploration target. (see Discussion below).

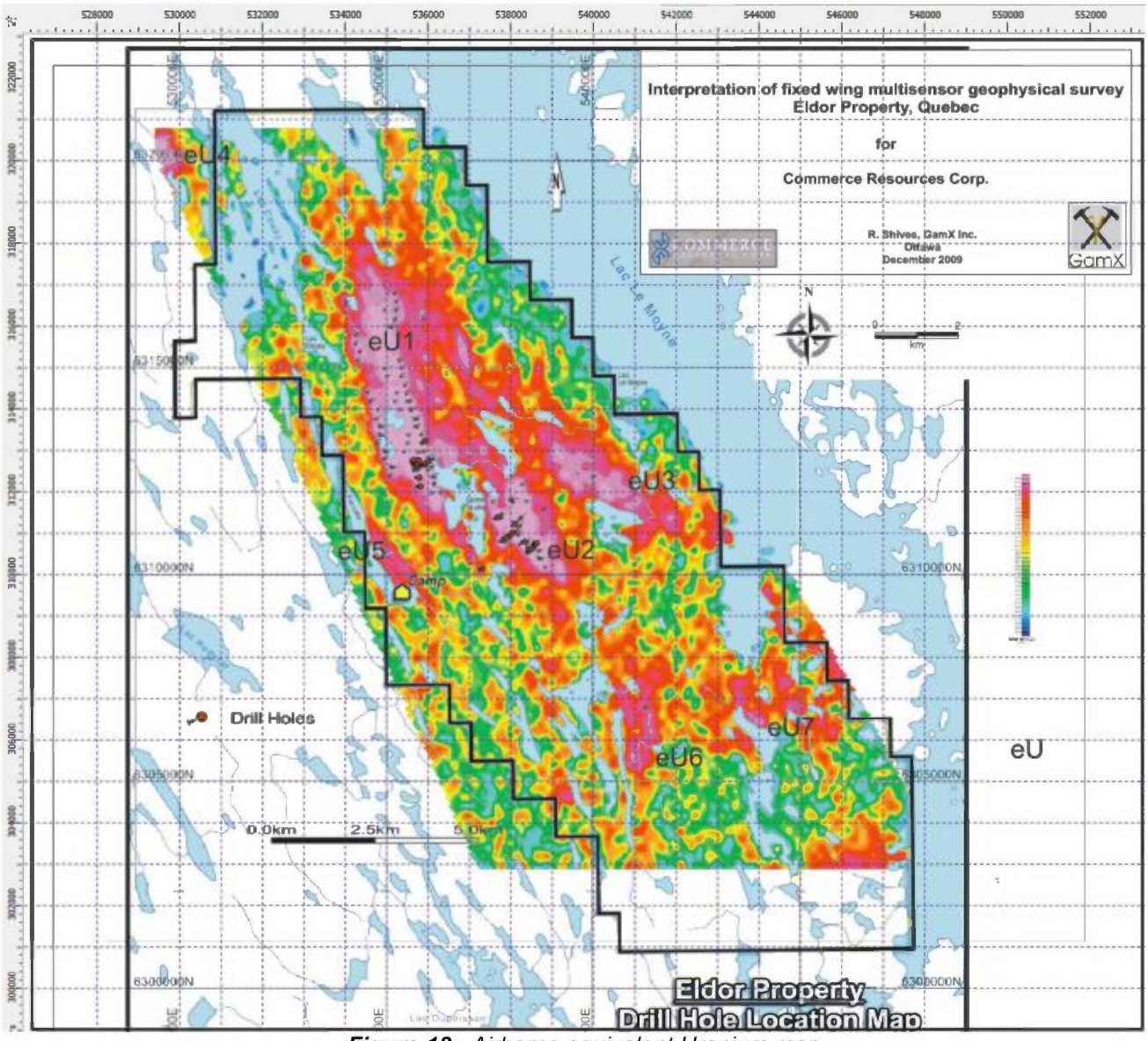

Figure 18. *Airborne equivalent Uranium map.*

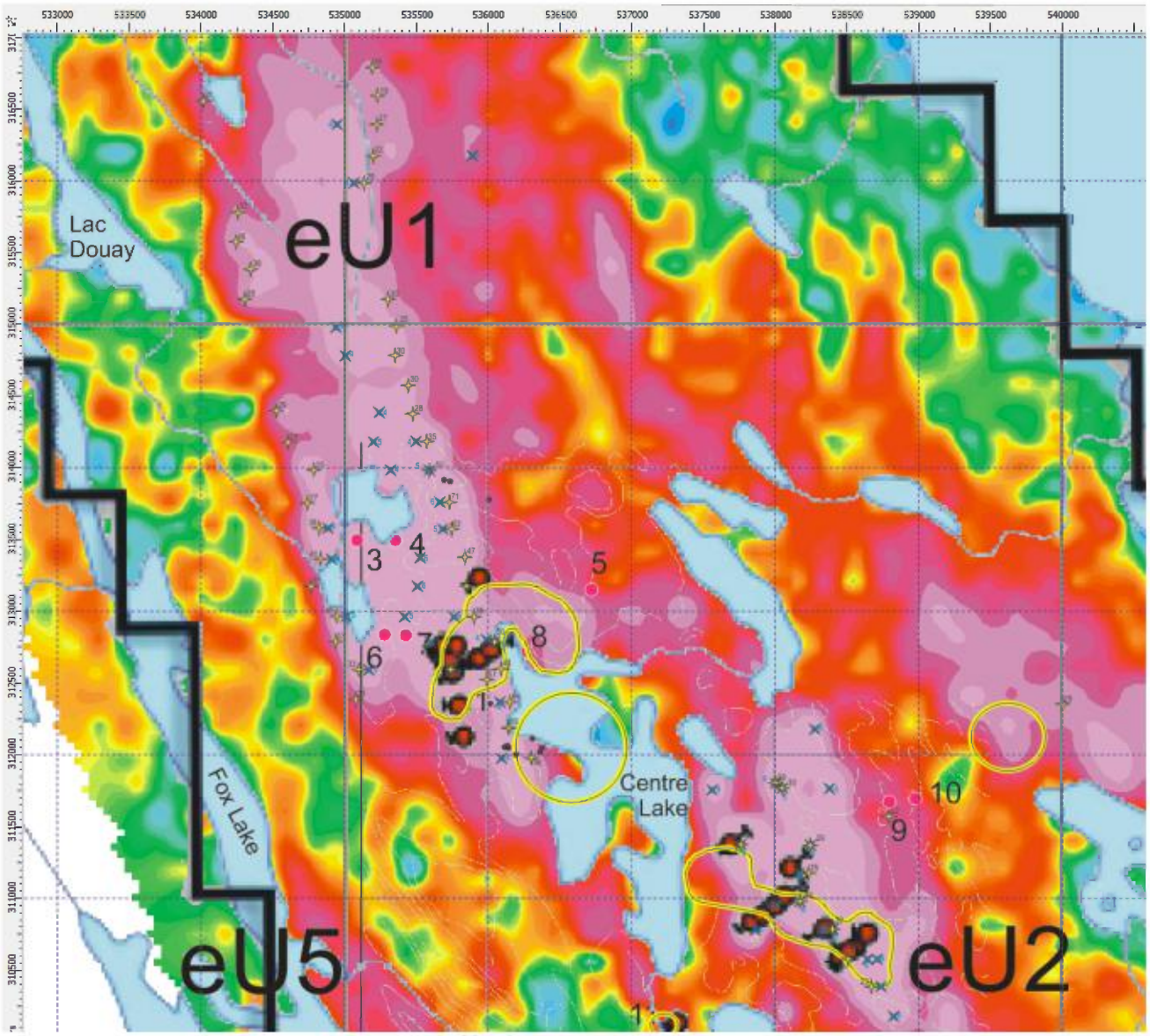

Figure 19. *Airborne eU map zoomed*

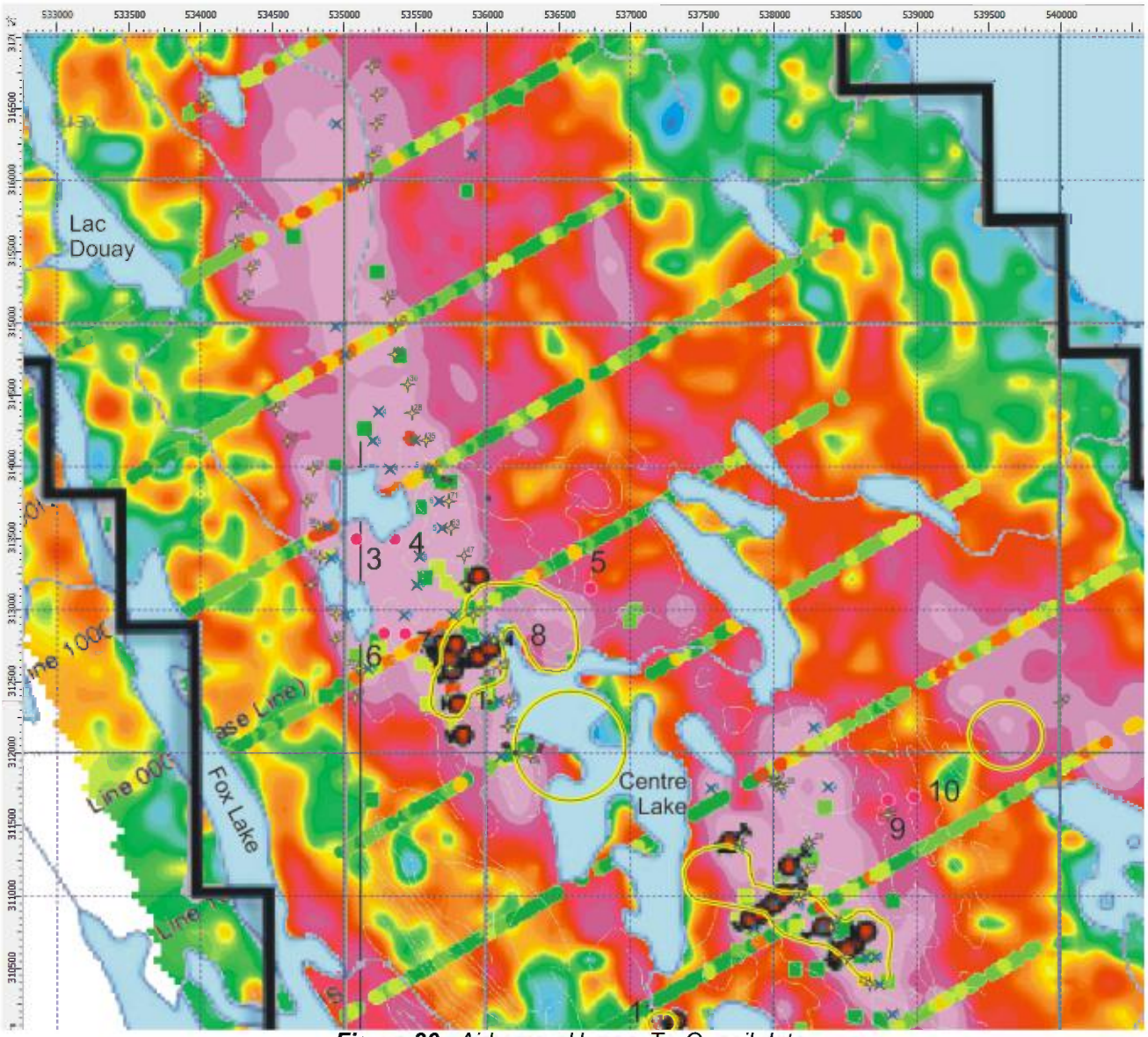

Figure 20. *Airborne eU map, Ta_2O_5 soil data*

5.2.3 equivalent Thorium (eTh) map

The airborne thorium values are dominated by the high values associated with the carbonatite, and concentrations associated with felsic host rocks appear only moderate. For example, the rhyodacitic unit along the eastern Fox Lake shore, east of the exploration camp, contains 6-10 ppm eTh (gridded values), while the carbonatite ranges from 40 to 80 ppm (gridded values). The continuity of the eTh trend interpreted as "rhyodacite" is impressive, extending roughly 10 km, following the eastern shore of Fox Lake and folding at the north end of the lake (forms a canoe shape just south of 6316000N). A second fold in this unit (at 6314300N) may be a faulted version of the same fold.

Similar to the eU patterns, eTh anomalies interpreted as carbonatite-related define five areas, labeled eTh1 through eTh5). eTh1 is defined by two parallel 345 degree trends, roughly 900 meters apart. Relationships to eU1 patterns are discussed below.

Correlation of the airborne eTh patterns with soil and rock REE+Y and Nb2O5 values is striking, suggesting the eTh is a good proxy for those elements in the material on surface.

Possible up-ice (southern) origins for the eTh anomalies are similar to the eU anomalies, and again, each anomalous area appears to encompass the combined response of several parallel trends. The coincidence or eU and eTh is not surprising, given the coexistence of these two elements in the (mineralized) carbonatite phases drilled to date. As with the Blue River carbonatites, relative enrichment of eU with respect to eTh may provide vectors to Ta-enriched phases/zones. This is indicated by the drill core assays as discussed previously.

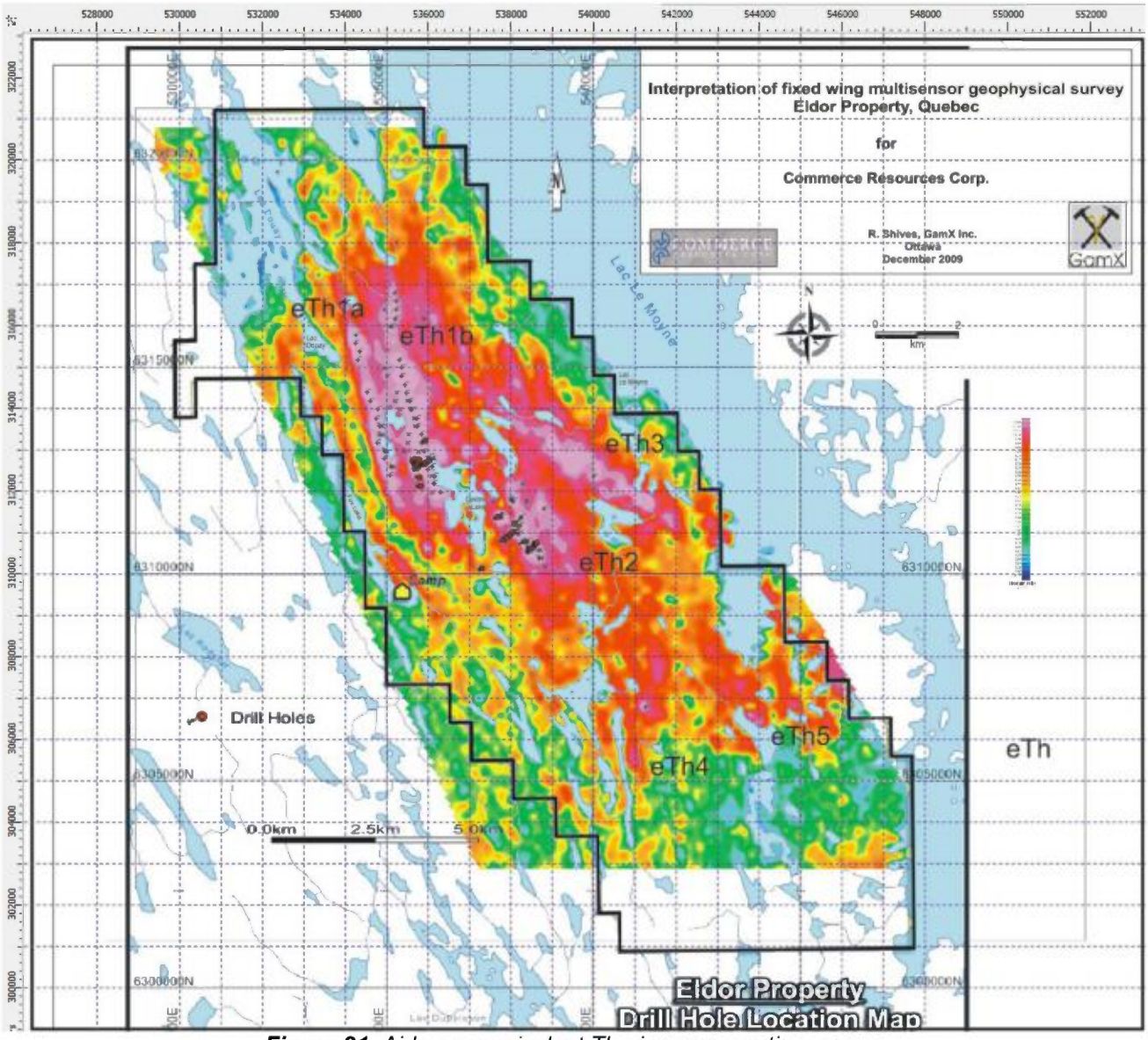

Figure 21. *Airborne equivalent Thorium map, entire survey*

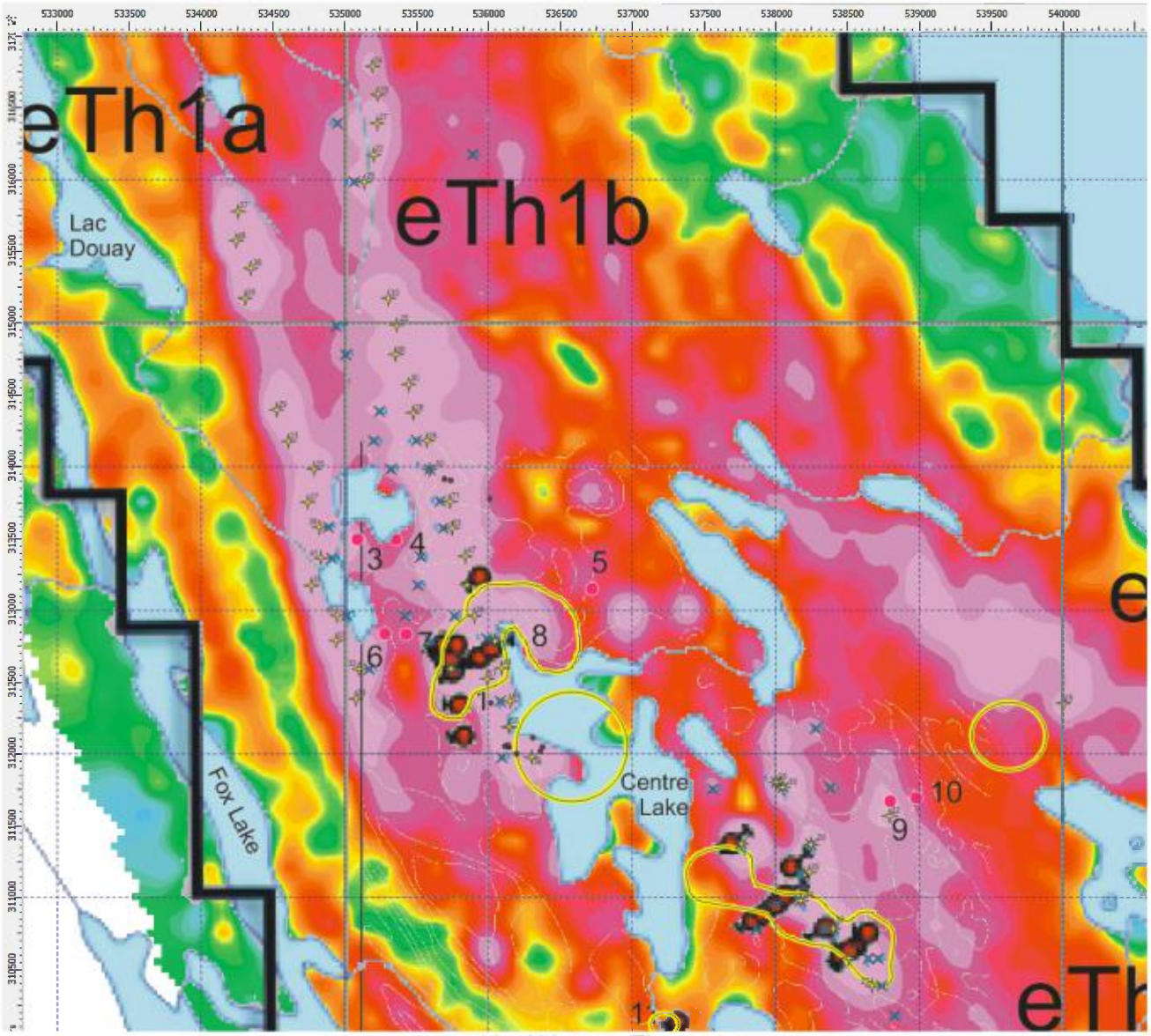

Figure 22. *Airborne eTh zoomed*

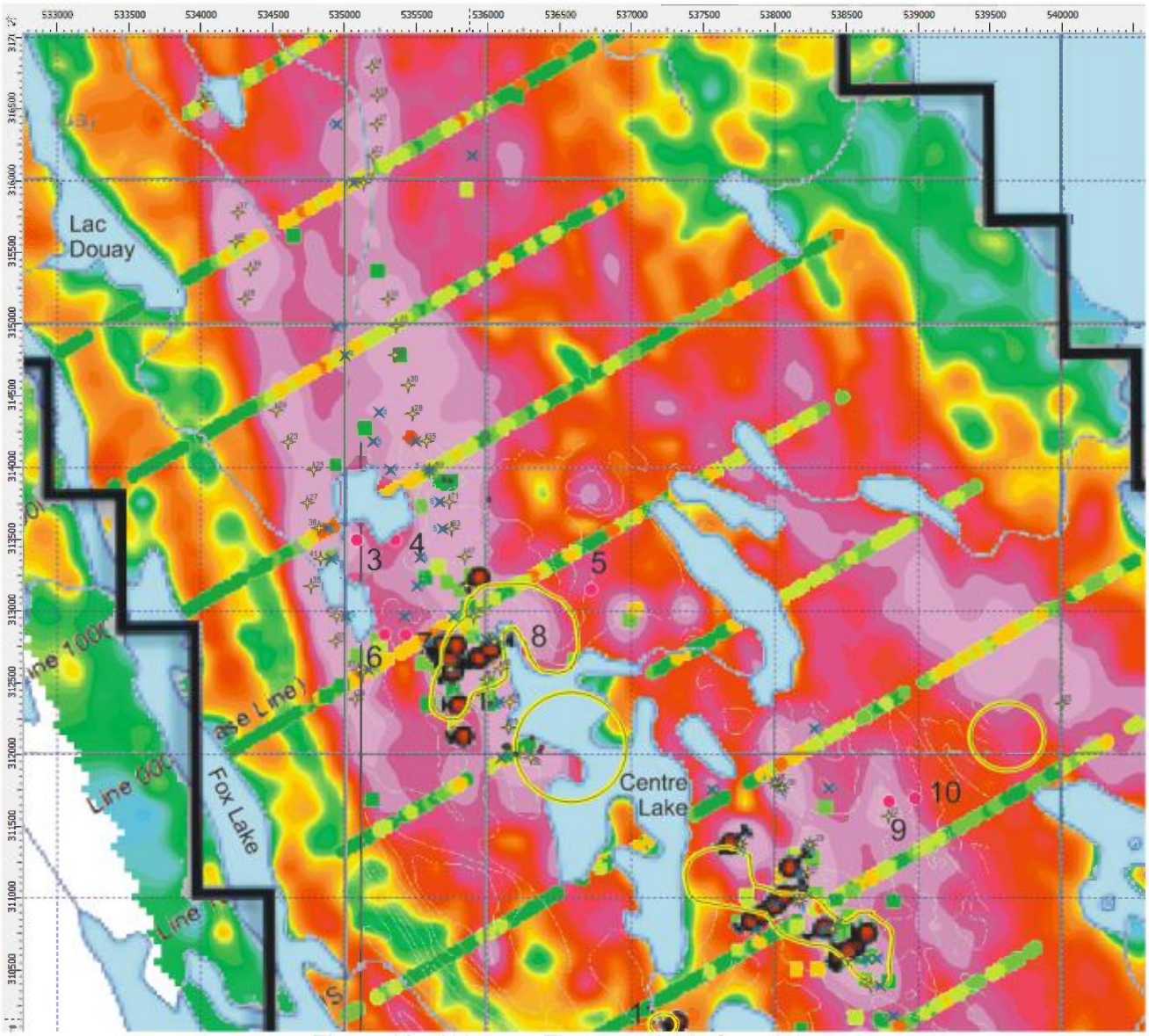

Figure 23. *Airborne eTh zoomed, Nb_2O_5 soil data*

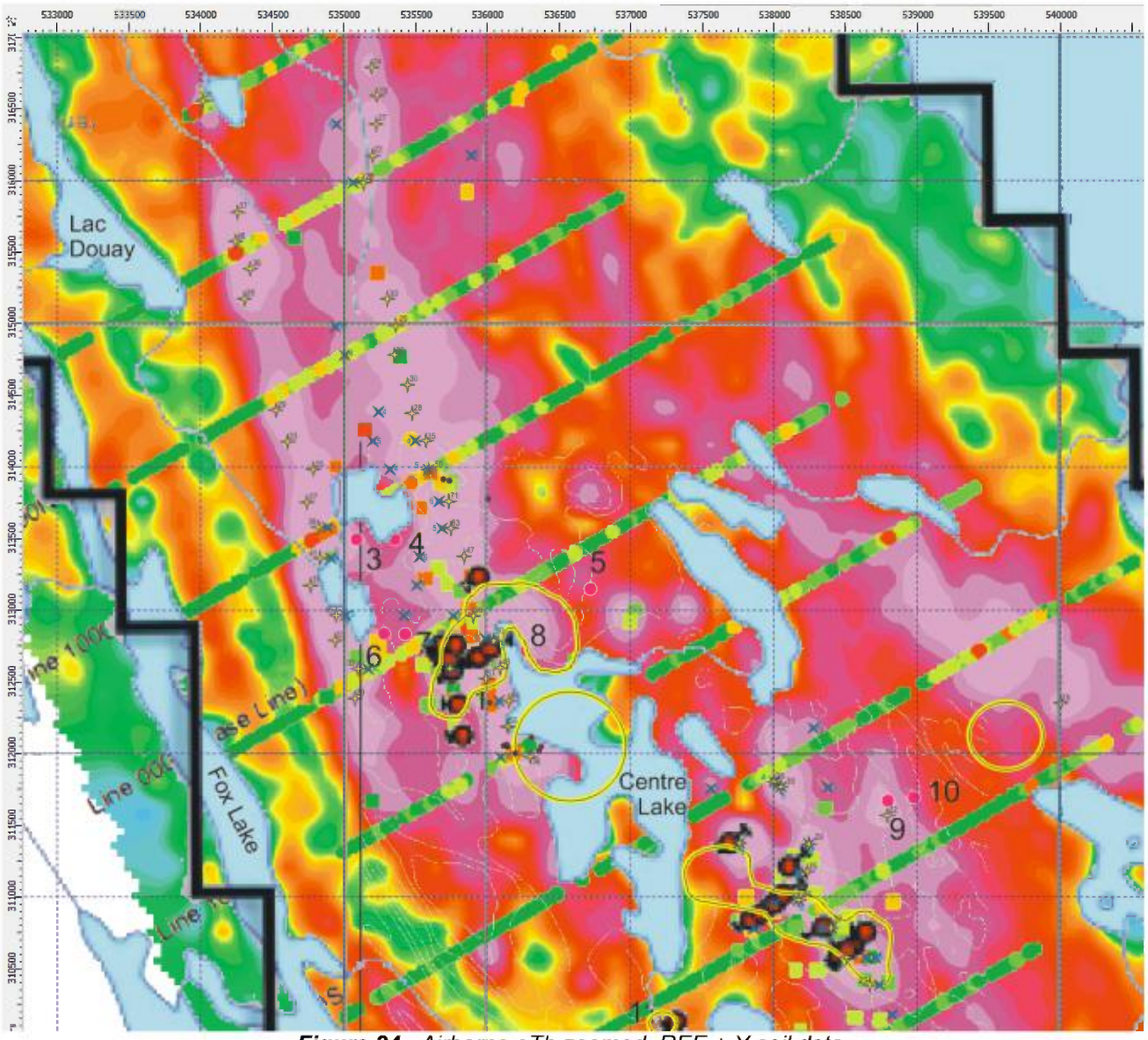

Figure 24. *Airborne eTh zoomed, REE + Y soil data*

5.2.4 eU/eTh, eU/K and eTh/K maps

As described above, the drill core assays indicate generally good correlation of uranium with Ta, and thorium with Nb, such that higher U/Th ratios derived from the drill cores assays correlate well with Ta. However, based on the eU/eTh ratio map for the survey, the ratio patterns are not well defined, are noisy, and eU/eTh highs are commonly unreliable (along lakes, where the statistical errors based on very low count rates cause "false" anomalies). This suggests that the ratio patterns must be used carefully, and cannot provide direct vectors to Ta-rich (or Nb-rich) areas without consideration of the individual eU and eTh values. Subtle "real" variations are apparent. The author interprets the lack of strong airborne eU/eTh ratio development to two factors: a) the lack of strong

partitioning in the carbonatitic magma (there definitely is relative variation between U and Th, but generally thorium enriched phases are also uranium enriched); and b) the suppression of subtle, valid ratio anomalies (they are visible) by much higher amplitude false eU/eTh anomalies in the low-count areas, which biases the gridded map colour distribution.

In stark contrast to the noisy eU/eTh patterns, the eU/K and eTh/K ratios provide intense, well defined anomalies, delineating relative (to K) enrichments in the three main areas (NW-Ashram, SW, and new eastern areas). Very strong eTh/K and eU/K anomalies are also produced over the two southern areas (labeled eTh4 and 5, and eU6 and 7, respectively). Although the amplitude of related eTh and eU values in the southern areas is less than in the known zones to the north, they represent valid exploration targets that should be investigated, perhaps on a lower priority basis.

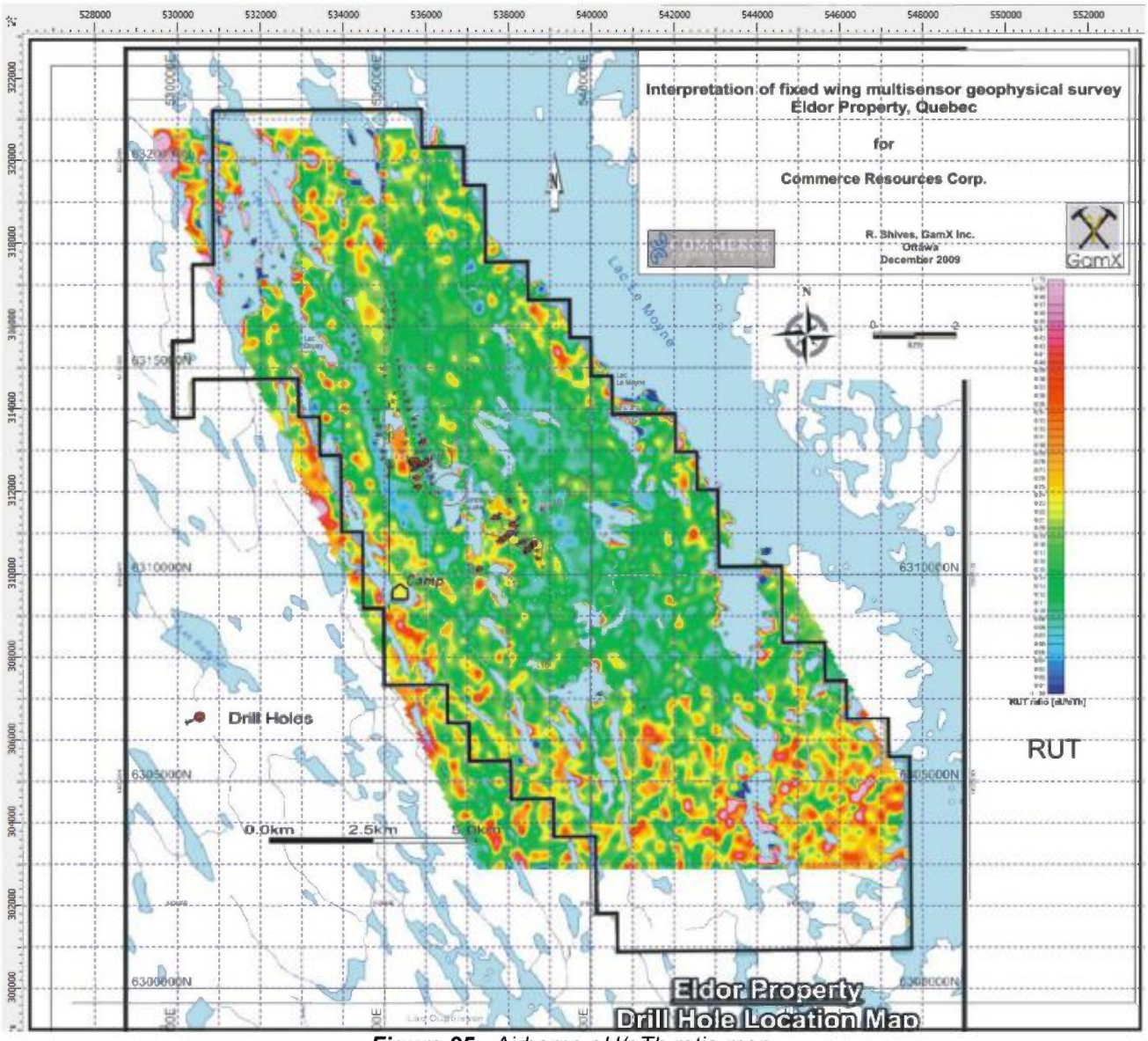

Figure 25. *Airborne eU/eTh ratio map*

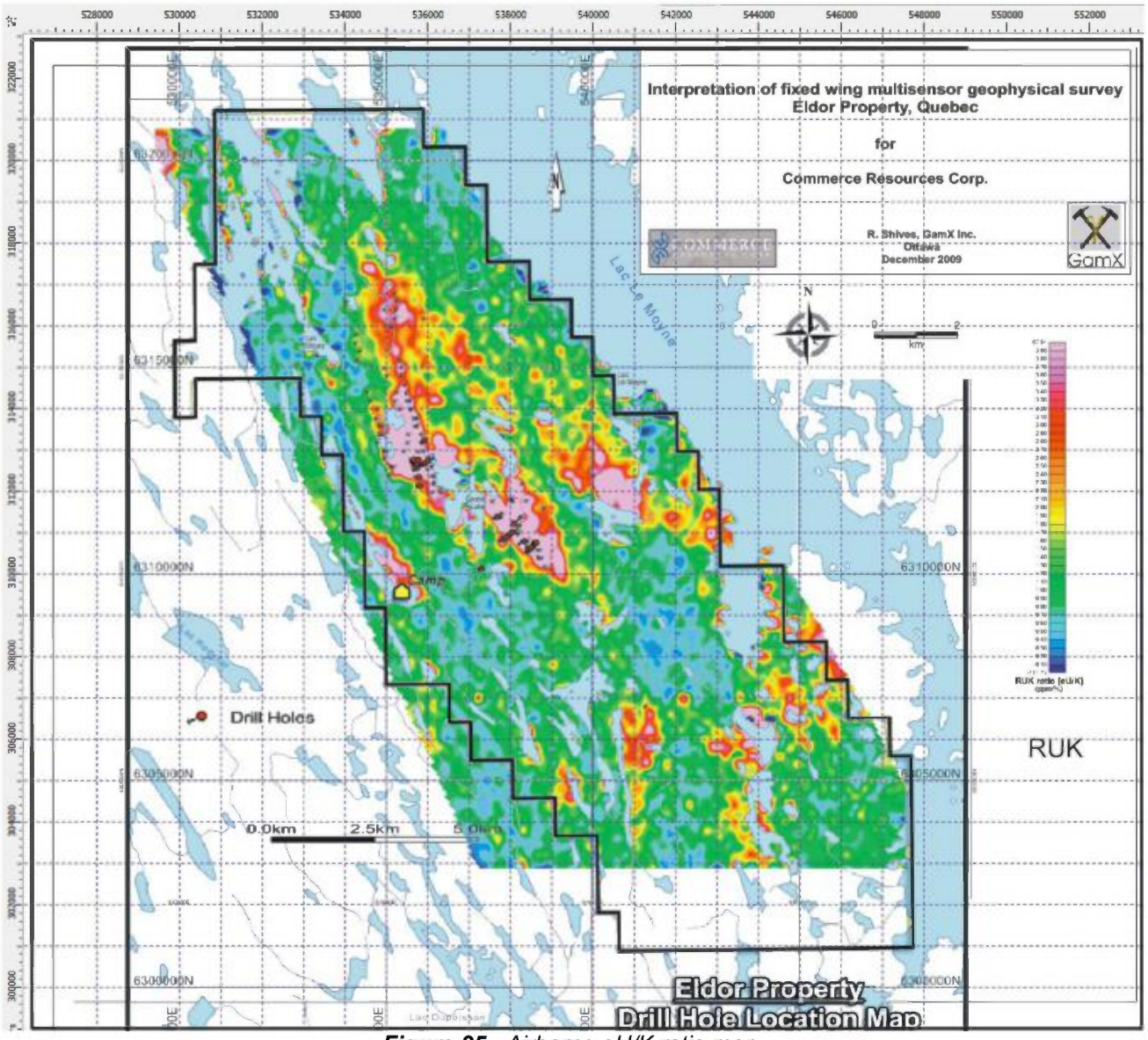

Figure 25. *Airborne eU/K ratio map*

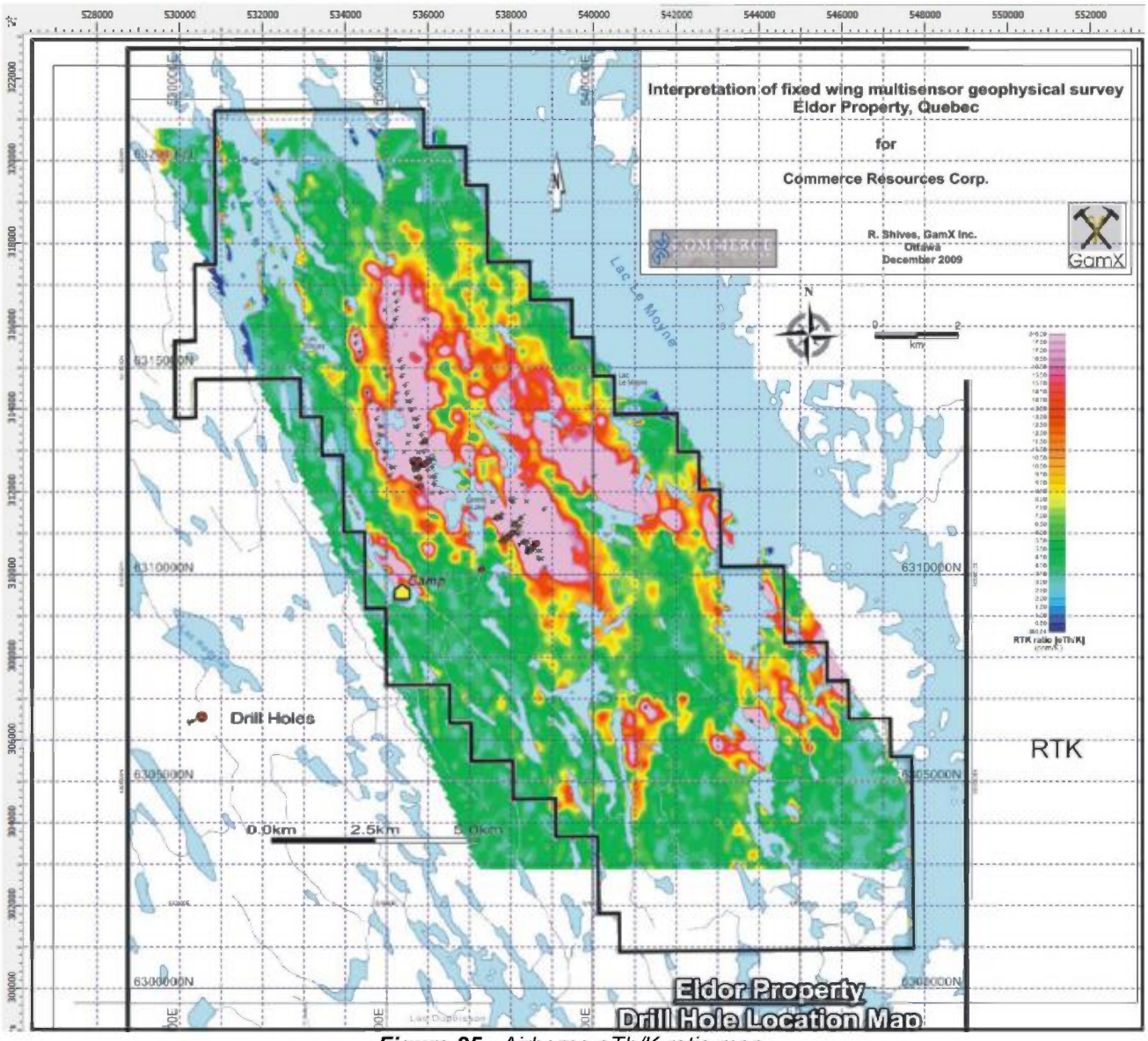

Figure 25. *Airborne eTh/K ratio map*

5.2.5 Ternary radioactive element (K-eU-eTh) map

The ternary map supplied by Abitibi was created using the GeoSoft approach, which uses a red-blue-green colour-mapping approach to show the relative variation of K, eU,eTh, respectively. While similar in concept to the "GSC ternary mapping method", the GeoSoft approach produces a murky map, where high total count areas (with high radioactivity) appear white. Thus, high eU areas may appear white, as do high eTh or high K areas, making it difficult to determine which of the three elements (or combination thereof) is responsible for the radioactivity high.

The following image depicts the "less desirable" Abitibi ternary image:

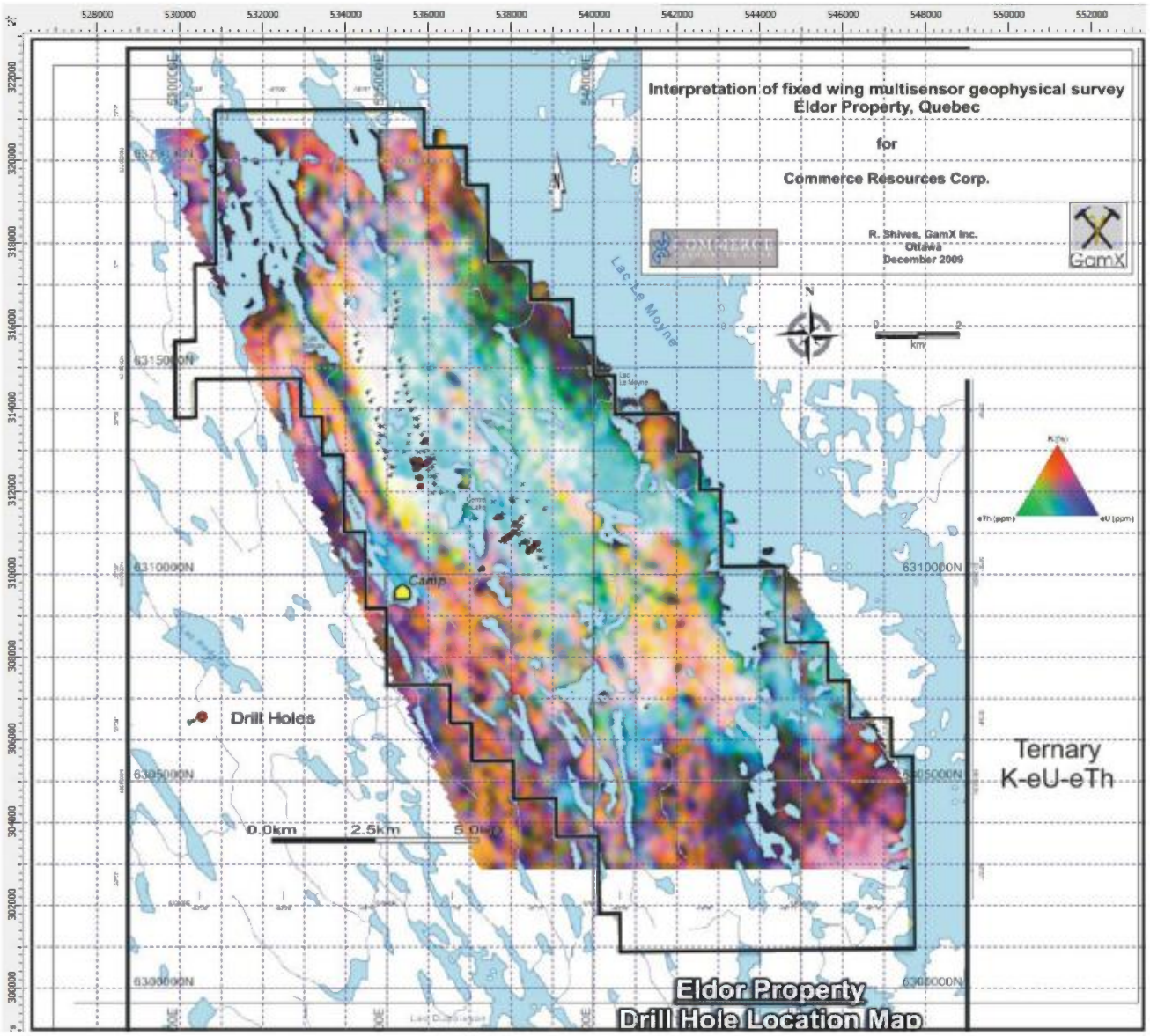

Figure 28. *Abitibi Ternary map*

The preferred GSC ternary mapping approach is cyan-magenta-yellow based (CMY, vs RGB) and creates intense hues based on the relative concentrations, such that high eU (relative) will appear as intense cyan, eTh will appear deep yellow, and high K will appear as strong magenta hues. This approach has been applied by the author, resulting in the following "more desirable" image:

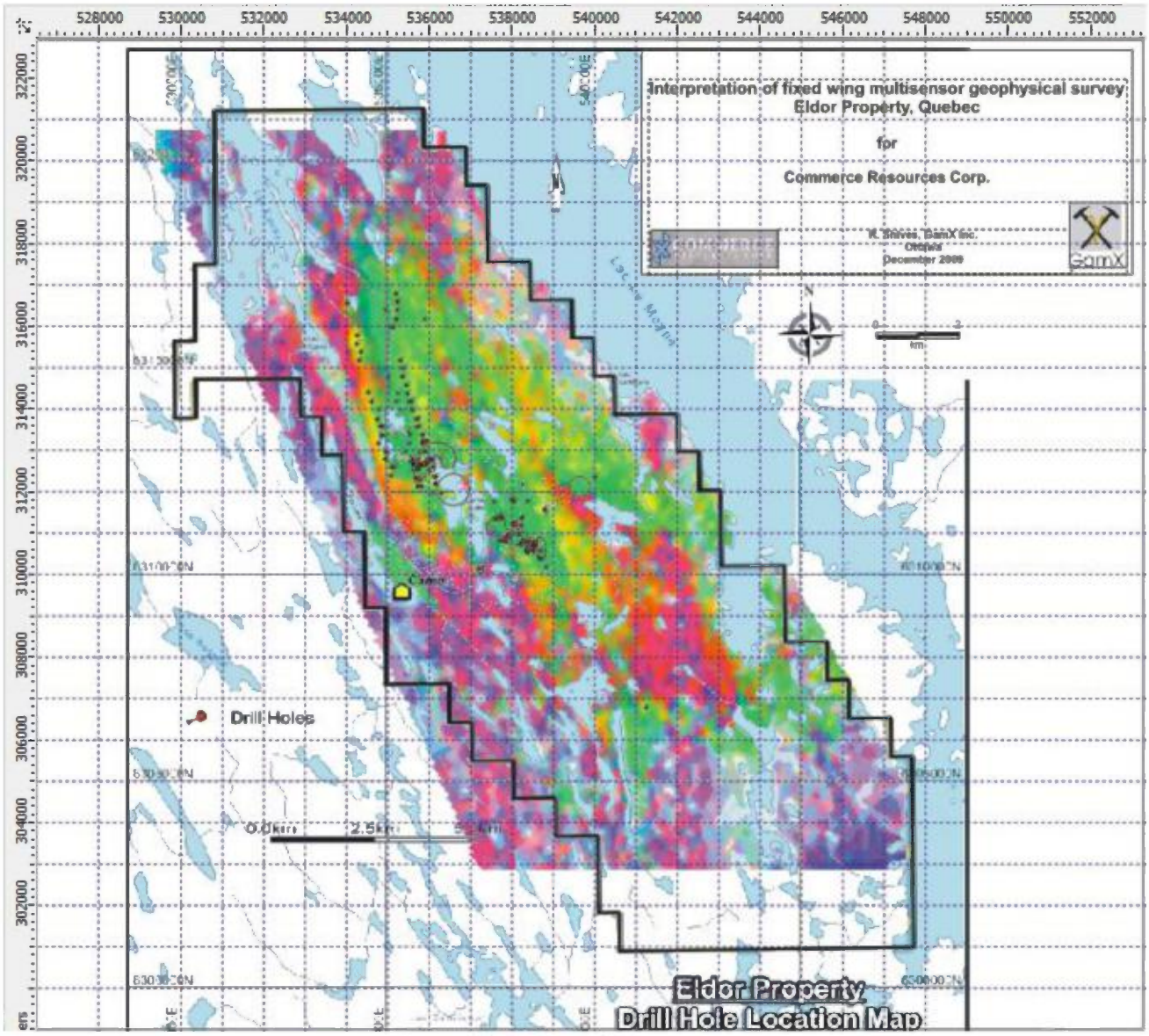

Figure 29. *GSC style Ternary map*

The colour distribution better defines radioactive element contrasts, relative to the Abitibi version.. The lack of intense blue (uranium-only) hues within the known carbonatite areas accurately reflects that the eU is generally accompanied by eTh, resulting in greenish colours. Pure yellow areas relate to eTh-dominated signatures. These are better shown on the zoomed version of the GSC ternary image, below. Appropriately, the yellow plus symbols (eTh anomalies picked form the detail

flight line profiles) lie along yellow trends on the ternary map, and the blue x symbols (eU picks from the profiles) overlie green or blue-green trends.

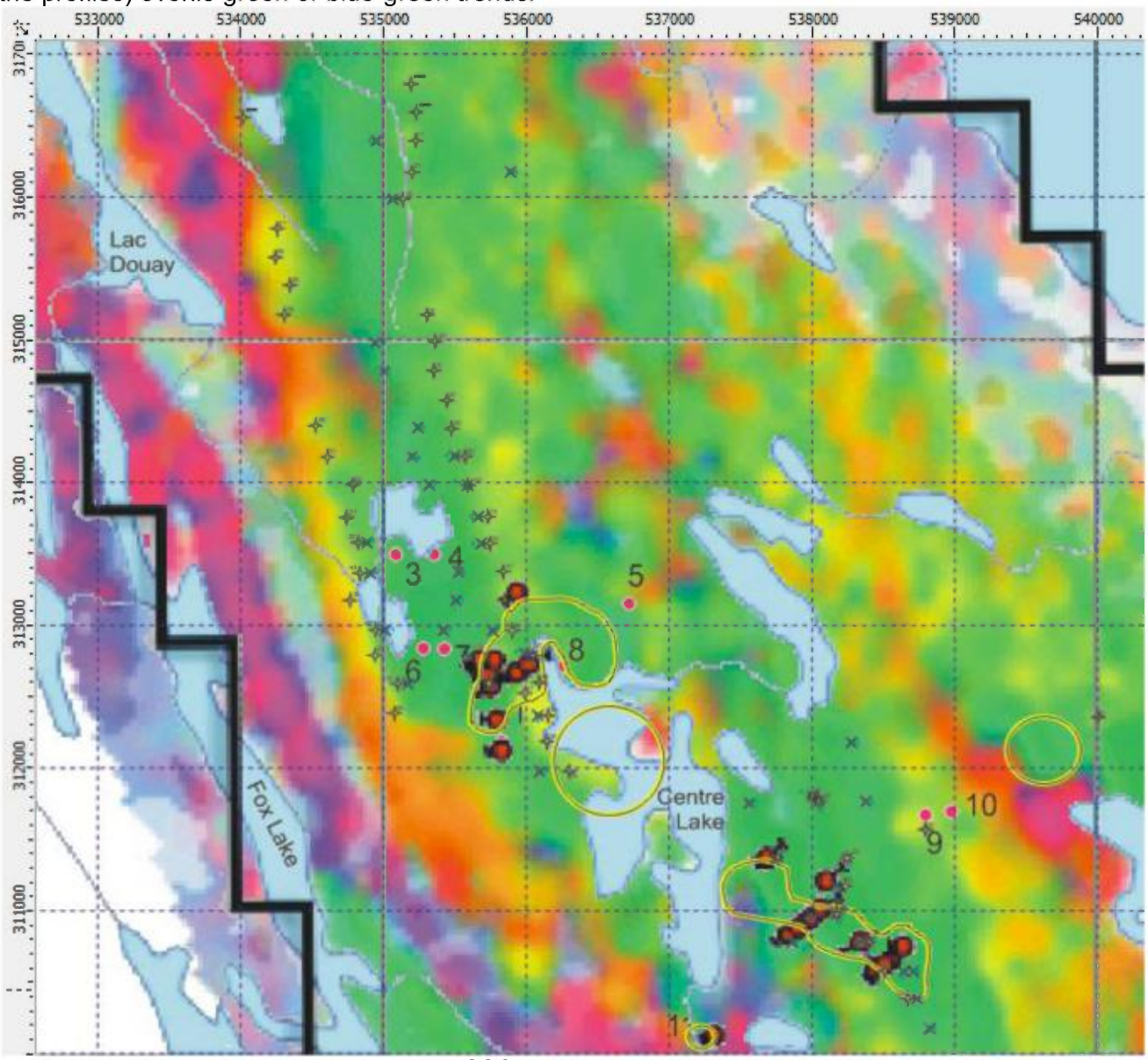

Figure 30. *GSC style Ternary map, zoomed*

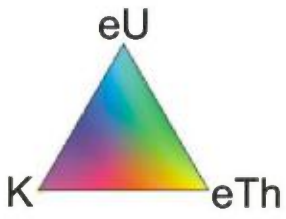

5.2.6. Stacked Profile Data

As discussed above, the gridded map presentations inherently smooth the data. Improved interpretation is possible using the detailed information as collected along the flight lines. The figure which follows illustrates one example that shows several features (labeled) including the responses over drilling in the NW Zone, where eTh and eU patterns are different. The west side of the anomaly has BOTH eU and eTh, and this suggests the drilling on that side may have encountered more Ta mineralization than the eastern side, which is less enriched in eU (airborne values), and thus may have relatively high Nb, with less Ta. (This interpretation has not been verified by the author.)

The flight line passed to the north of the new carbonatite outcrops discovered recently along the eastern side of the intrusive complex. Note the eTh highs here, again, implying possible carbonatite source material (already proven) which may be relatively enriched in Nb and REE + Y.

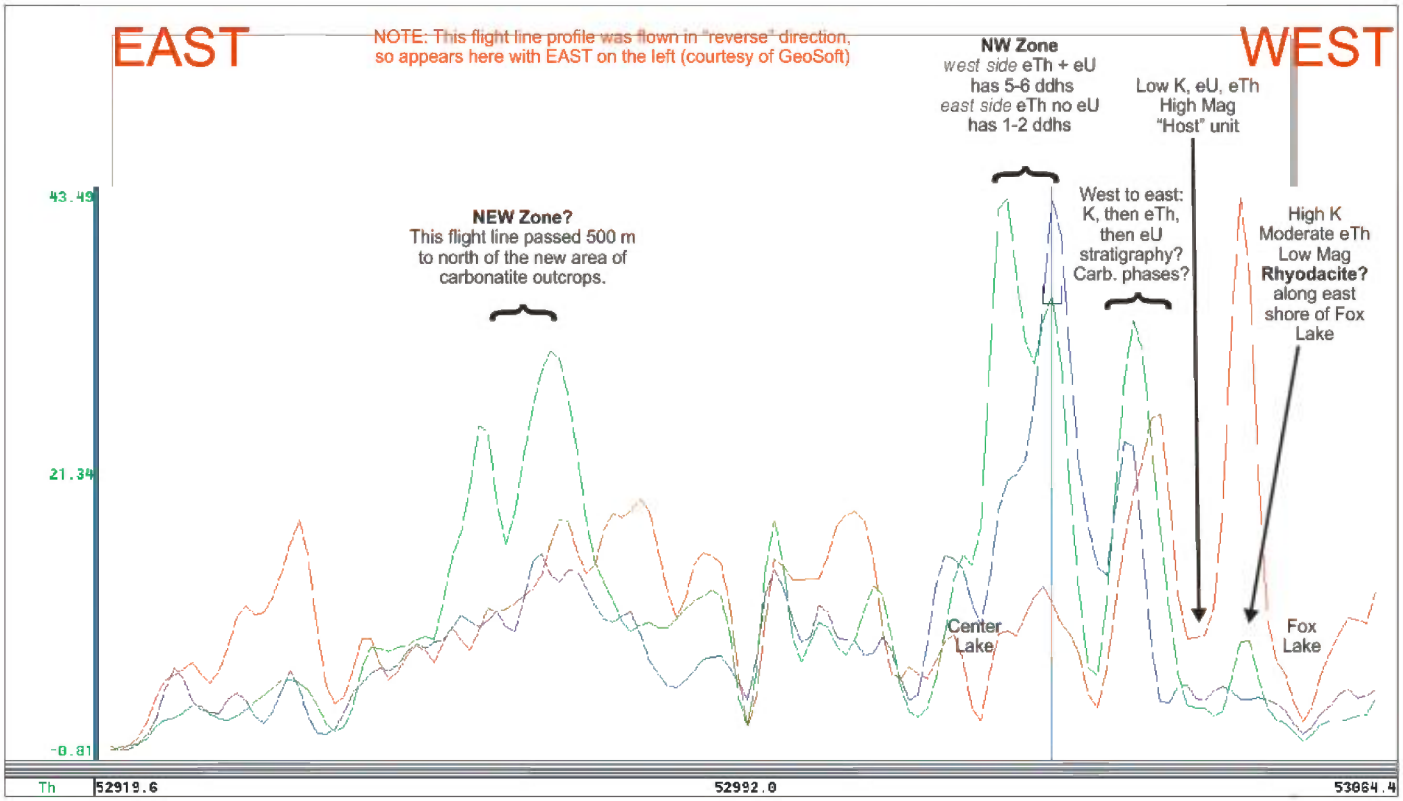

This type of stacked profile analysis should be conducted in all areas of interest. Dahrouge/Commerce can readily view the stacked profile data provided by Tundra, using the free GeoSoft Oasis viewer. An example of this type of image is provided below.

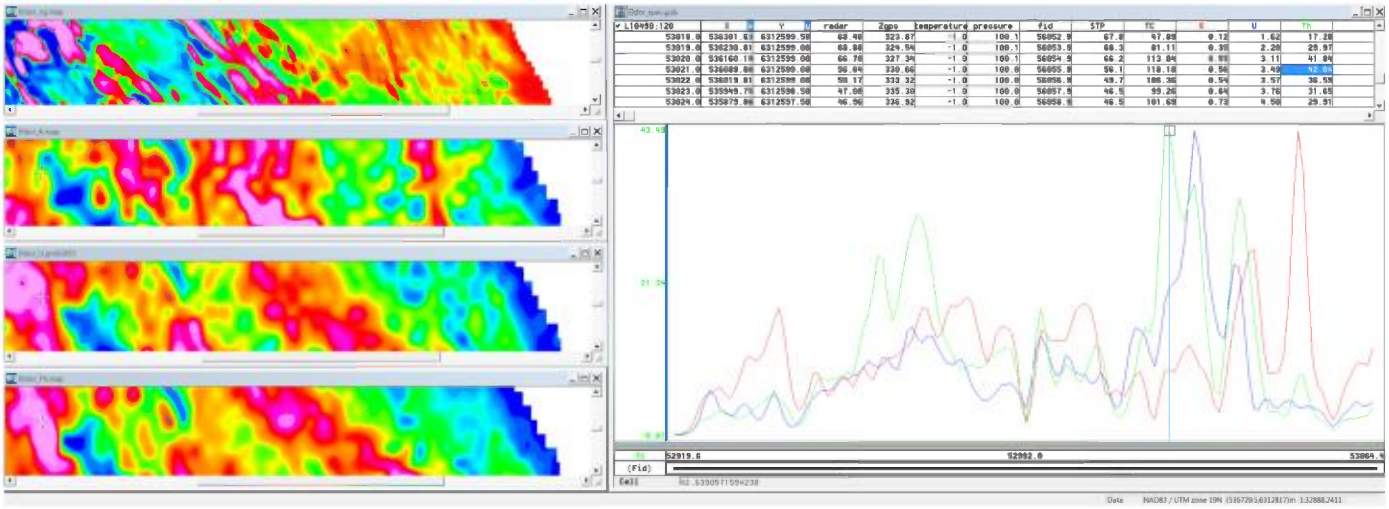

5.3 Target Picks: Top 30

Statistical analysis of the airborne spectrometric line data was conducted by the author to define the top 30 highest values for each of the three radioactive elements. These are tabulated below, grouped by eTh, eU and K sections, each with corresponding Total Count TC) values, and each section organized from highest value to lowest. Corresponding UTM coordinates (NAD83 Zone 19) for each data point provide potential targets to locate the specific anomalies on the ground, for possible follow-up.

The highest eTh measured airborne values (ranging from 42.7 to 86.1 ppm eTh) are highlighted in yellow. Highest eU values (the middle section of the table) are highlighted in blue. Note that six of the highest eTh values are included with the top 30 eU values. Highest K values are highlighted in pink in the right hand section.

	A	B	C	D	E	F	G	H	I	J	K	L	M	N	O	P	Q	R	S	T	U
1	Commerce Eldor Carbonatite Project, Quebec																				
2	Airborne Survey Interpretation																				
3	GamX Inc Selected Targets (based on eTh, eU and K responses)																				
4																					
5		NAD83 Zone 19		Top 30 eThorium responses					NAD83 Zone 19		Top 30 eUranium responses					NAD83 Zone 19		Top 30 Potassium responses			
6	Line	Easting	Northing	TC	K	U	Th	Line	Easting	Northing	TC	K	U	Th	Line	Easting	Northing	TC	K	U	Th
7	L10480	536153	6312366.5	208.86	0.68	3.63	86.12	L10430	537760	6311376	153.84	0.29	8.73	45.83	L10440	539664	6311571	70.85	2.80	1.01	9.61
8	L10480	536082	6312368	190.37	0.58	4.07	76.49	L10430	537830	6311375	149.79	0.47	8.26	43.95	L10500	534112	6312786	67.77	2.80	1.00	8.13
9	L10550	535732	6313760	201.38	1.11	5.57	71.49	L10410	538172	6310978	133.00	0.78	7.54	35.53	T19020	534009	6313149	65.01	2.79	0.34	7.93
10	L10480	536224	6312366.5	160.37	0.54	2.86	65.69	L10490	535740	6312594.5	128.42	0.70	7.13	35.21	L10230	541535	6307384	74.66	2.79	1.13	11.22
11	L10550	535664	6313761	186.48	0.97	5.91	64.31	L10410	538240	6310979.5	129.48	0.74	7.11	35.42	L10250	541523	6307795	76.50	2.72	1.02	12.88
12	L10540	535747	6313573.5	176.34	0.93	4.88	63.12	L10410	538103	6310976.5	121.01	0.89	6.75	31.24	L10440	539739	6311572	70.14	2.72	1.14	9.70
13	T19030	535991	6312523.5	150.73	0.72	3.17	57.44	L10490	535669	6312593	112.39	0.60	6.65	29.77	L10250	541588	6307795	75.46	2.72	0.89	12.75
14	L10550	535800	6313760	163.04	1.17	4.17	56.75	L10420	538166	6311175	129.25	0.90	6.63	35.31	L10490	534245	6312583	64.72	2.72	0.66	8.38
15	L10540	535808	6313574	156.87	0.93	4.45	55.06	L10420	538232	6311175.5	129.37	0.94	6.52	35.48	L10530	533933	6313382.5	62.56	2.70	0.69	7.37
16	L10470	536144	6312188	142.38	0.72	3.02	55.01	L10380	538737	6310386	95.03	0.71	6.52	21.21	L10510	534065	6312978	62.64	2.69	0.73	7.45
17	T19030	535990	6312454	137.51	0.68	2.49	53.24	L10420	538099	6311173.5	116.66	0.83	6.25	30.97	T19020	534009	6313081.5	63.73	2.68	0.50	7.68
18	L10540	535685	6313573	150.28	0.82	4.90	51.41	L10520	535508	6313175	86.02	0.56	6.24	18.45	L10270	541523	6308171.5	67.13	2.65	0.60	9.87
19	L10480	536012	6312369.5	134.74	0.57	3.73	50.27	L10380	538670	6310384.5	98.05	0.80	5.98	23.38	L10250	541652	6307794.5	75.40	2.64	0.93	13.16
20	L10500	536046	6312786.5	144.29	0.48	5.27	50.24	L10410	538308	6310981.5	114.87	0.65	5.94	32.54	L10260	541606	6307978	68.85	2.63	1.14	9.76
21	L10560	535591	6313982	144.44	0.78	4.74	49.74	L10550	535664	6313761	186.48	0.97	5.91	64.31	L10210	543348	6306990.5	64.17	2.63	0.63	8.57
22	T19030	535990	6312592.5	136.49	0.77	3.78	48.42	L10390	538710	6310576	94.20	0.74	5.85	22.18	L10260	541536	6307978.5	70.97	2.60	1.05	11.21
23	L10470	536219	6312187.5	121.18	0.38	2.82	47.86	L10490	535810	6312596	117.66	0.78	5.84	33.23	L10270	541591	6308171	65.98	2.60	0.67	9.59
24	L10500	535982	6312786.5	141.15	0.73	4.93	47.76	L10520	535439	6313175	78.02	0.45	5.80	16.63	T19020	534009	6316065.5	68.13	2.60	0.98	9.51
25	L10530	535839	6313378	137.60	0.85	4.28	46.72	L10430	537690	6311376	104.37	0.27	5.80	30.66	L10620	532550	6315174	67.29	2.58	1.13	9.04
26	L10640	534245	6315576	137.29	1.56	2.87	46.06	L10390	538643	6310576.5	101.28	0.88	5.79	24.86	L10230	541604	6307382.5	73.32	2.58	1.26	11.67
27	L10430	537760	6311376	153.84	0.29	8.73	45.83	L10530	535528	6313373	95.67	0.90	5.65	21.87	T19020	534009	6313216.5	61.51	2.58	0.59	7.12
28	L10510	534946	6312966	134.53	1.10	3.99	44.71	L10550	535732	6313760	201.38	1.11	5.57	71.49	T19020	534008	6315996	66.37	2.57	1.02	8.75
29	L10430	537830	6311375	149.79	0.47	8.26	43.95	L10430	537899	6311374	108.13	0.67	5.53	30.35	L10510	533997	6312978	59.17	2.56	0.86	6.53
30	L10500	535919	6312786.5	128.61	0.78	4.01	43.90	L10420	538299	6311176.5	111.25	0.95	5.51	29.74	L10520	533949	6313169	62.59	2.55	1.00	7.19
31	L10550	535595	6313762.5	135.37	0.72	5.16	43.75	L10530	535605	6313375	103.61	0.87	5.44	26.66	L10250	541458	6307795	73.13	2.54	1.08	12.45
32	L10560	535525	6313982.5	129.89	0.70	4.71	43.55	L10530	535450	6313371	86.67	0.86	5.34	18.66	L10210	543278	6306989	62.00	2.50	0.54	8.76
33	L10530	535761	6313377	134.71	0.95	4.66	43.54	L10520	535576	6313175.5	88.18	0.72	5.31	20.98	T19020	534009	6313014	61.81	2.49	0.91	7.06
34	L10560	535657	6313982	128.57	0.95	3.77	43.37	L10390	538575	6310576.5	104.62	0.82	5.28	28.46	L10520	534020	6313170.5	60.60	2.49	1.03	6.75
35	L10520	535850	6313177	125.53	0.93	3.41	43.04	L10500	536046	6312786.5	144.29	0.48	5.27	50.24	L10260	541675	6307978	64.60	2.47	1.16	8.71
36	L10510	535013	6312965	133.90	0.92	4.99	42.72	L10550	535595	6313762.5	135.37	0.72	5.16	43.75	L10240	541546	6307574	78.93	2.44	1.55	14.50

6.0 Discussion

The apparent low in all three radioactive elements over the Ashram Zone may be related to the masking affect of Centre Lake and surrounding wet ground, rather than a decrease in bedrock concentrations under the lake.

The almost complete lack of correlation between the eU and eTh patterns and the aeromagnetic patterns cannot be explained if we assume the radiometric trends overlie their bedrock sources in all instances, unless the radiometric trends relate to post-folding, post-main intrusion (so "late") brittle, linear N-S (345 degrees) faults into which either dikes of carbonatite have intruded, or, the elements have been remobilized. It is difficult to place these potential structural breaks into the aeromagnetic patterns.

Alternatively, if we assume that glacial dispersion has indeed affected the distribution of radioactive elements (and many other elements) at Eldor, then a cautious approach would restrict initial follow-up to the "heads" of the anomalies located at their southern limits. According to D. Smith (pers comm.) this approach was used to trace NW zone results southerly, defining the Ashram Zone.

If we also assume that the 345 degree direction is valid, then each eU anomaly can be interpreted as the combined effect of subparallel trends, each with their own point of origin. Thus eU1 would extend from Centre Lake (or west of the lake) along 345 degrees through the easternmost drilling in the NW Zone, and continue in that direction for another 4+ km, subject to glacial dispersion affects. A second parallel trend would occur roughly 300m to the west (and this trend has been followed closely by where the westernmost series of 7 or so drill holes), originating near the NW zone and heading northwards. A third parallel trend would be located another 550 m to the west.

Alternate explanations of possible dispersion patterns are possible, such as a single, larger bedrock source (an enriched phase of the carbonatite) at the "head", which has been drawn out into multiple trains, perhaps due to the distribution of pre- and syn-glacial topographic knobs (availablilty of anomalous bedrock sources).

The airborne thorium patterns also lie along the 345 degree trend in anomaly eTh1. Again, do these represent underlying bedrock lithological trends (which cross both mapped bedrock geology and the magnetic patterns along breaks in the mag) or are they better explained by glacial dispersion? Note that analysis of the detailed stacked profiles along the entire length of this anomaly (eU1 and eTh1) indicate displacement of the eU and eTh maxima along the flight line profile, such that eTh forms outer borders defining the east and west edges of the anomaly, and eU forms three subparallel trends between the eTh highs. The line-to-line consistency of these relationships is remarkable – would glacial dispersion alone maintain this pattern so consistently, or is a local bedrock source along the anomaly, a more plausible explanation?

7.0 Conclusions

- The airborne geophysical survey completed in 2007 over Commerce Resources Corp.'s Eldor Property by Tundra Airborne Survey provides quantitative gamma ray spectrometric and magnetic information which can been interpreted at regional, property and local (showing) scales. The data is of good quality.

- A multi-layered database constructed by the author using CorelDraw X4 allows spatial comparison of airborne and available ground data, has been used to interpret the airborne survey and offers a solid base to add future information provided through Commerce, if desired.

- Map views of the aeromagnetic data reflect regional, host-rock patterns and possible deposit-specific signatures, either as magnetic total field highs (NE and SW Zones, and possibly the new Eastern zone, and new southern 2 zones?) or as lows (Ashram and Star Trench Zones). Magnetic susceptibility data has not been collected on outcrops or drill cores to date, inhibiting interpretation somewhat.

- The radioactive element data define a few anomalies interpreted as lithological trends in the host volcan-sedimentary rocks. Patterns within the mapped extent of the carbonatite complex, however, sharply define three main areas and possibly two additional, lower priority new areas of exploration interest.

- Glacial modification of bedrock-associated radiometric anomalies, through down-ice dispersion to the north (bearing 345 degrees) has been interpreted. Variable distances of dispersion are possible, from 1 to 8 km, but an alternative explanation is postulated, where anomalous source rocks occur, at least in part, along the airborne trends.

- Both aeromagnetic and radiometric data are best viewed in detail using the stacked profiles derived directly from the flight line data. This is less filtered than the gridded presentations, allowing spatial resolution of separate eU and eTh and K maxima. In all zones, parallel eU and eTh trends can be discerned from the profiles. In the NW zone, radioelement zoning is indicated by a central eU core and peripheral eTh to the east and west.

- The data support improved exploration targeting in known, drilled areas (extension to known zones) and in new untested areas, including the Eastern outcrops, and two southern areas.

- A Top 30 list has been provided for each of eTh, eU and K airborne values. While these are not expected to provide direct vectors to Nb and or Ta occurrences, the strong correlations established using drill core assays and through comparison of airborne patterns with soil and

bedrock chemistry, suggest they may offer prospecting targets. UTM coordinates have been provided.

8.0 Recommendations

1. On-going Data Integration.

This report has been based on integration of various information supplied to the author by Dahrouge. Results indicate some valuable new ideas and targets. Cooperative re-interpretation and feedback with the author and Commerce/Dahrouge representatives is recommended, integrating new 2010 field information. The current report indicates potential in several areas.

2. Additional Ground Work

Follow-up should include initial prospecting in general areas of interest, focused at specific locations determined by additional scrutiny of the existing data. Work should include reconnaissance gamma ray spectrometry (vs. systematic grid surveys) to characterize the radioactive element signatures in each area. This work can be expected to extend the airborne targets between flight lines, will detect new areas of radioactivity, and will distinguish targets warranting further work. The latter should include systematic scint surveying, soil sampling and ground magnetic surveys similar to work previously conducted on the properties. The author welcomes possible field interaction with Commerce/Dahrouge staff in 2010 to conduct some of this recommended follow-up.

3. Magnetic Susceptibility

Given the importance of the aeromagnetic patterns as indicators of various magmatic carbonatitic phases, it is strongly recommended that all historical and future drill cores, and perhaps critical (mineralized) outcrop exposures, be measured systematically using modern MS meters. The data will support improved core logging, recognition of the "magnetic facies" represented by the various phases, and correlation of MS with mineralization. It will thus improve interpretation of the aeromagnetic data.

Respectfully submitted
April 12, 2010

R.B.K. Shives

P.Geo., President, GamX Inc

APPENDIX 15A: LIST OF SAMPLES COLLECTED FOR THIN SECTION WORK (CORE)

Values have been corrected for driller depth error (EC08-016-020)

Sample	Hole	Depth (m)	~Thin Section Length (cm)	Sample Decription	Reason For Selection	Interval Description		
						From	To	Remarks
68101	EC08-001	6.22	6.5	*Carb 4* - v f.g., r-blk streaks, dk gy dyke, fl (minor), py	INT - returned 1.01% REE+Y, highest in dataset	5.89	6.49	- late v.f.g. mass Carb dyke, fl frags at upper ctc (~40° to TCA)
68102	EC08-002	154.70	14	*Carb 2* - dyke, phyritic, mag	INT - mineralized Carb 1c, with 0.3% Nb and no Ta	154.00	163.00	-
68103	EC08-002	159.15	10	*Carb 1* - normal, homo, unidentified y-br diss min				
68104	EC08-002	162.35	9	Carb 2 - dyke, cr, mafic poor				
68105	EC08-002	188.55	13	Carb 3 - gr, mafic rich	INT - mineralized Carb 3	*187.90*	*188.70*	- grish alt. Carb 2 (c.g.). Up hole is f.g. gr-ish, streaky Carb 3 carb. Below is unaltered Carb 2 at ctc with Carb 3, altered by Carb 3. Cut by one Carb 3 vn
68106	EC08-002	198.40	8	Carb 2 - skeletal, mag (abnt), sul (minor)	INT - completely unmineralized Carb 2b	198.00	204.00	Skeletal textured Carb 2 well developed skeletal locally (198.05-198.80), 203.2-203.5 Silicocarbonatite clumps 199.1-199.75, Elsewhere mafics v c.g., pheno mag and gr-ish gy, overall mildly mafic rich. Significantly the interval contains much m.g.-c.g. phl and is relatively mag poor except in skeletal sections and v c.g. mafic clots. RA only 160-140 (bkgd 100) Pieces: @198.4 (68106) - skeletal, @ 199.8 (68107) - v c.g. gr-gy unidentified min, @201.2 (68108) - mag phenos, @203.25 (68109) - wk skeletal
68107	EC08-002	199.80	14	Carb 2 - mag (abnt), py (minor)	INT - completely unmineralized Carb 2b, v.c.g. gr gy unidentified min			
68108	EC08-002	201.20	6	Carb 2 - very similar litho to 68107	INT - completely unmineralized Carb 2b, Mag phenos			
68109	EC08-002	203.75	8	Carb 2 - similar litho to 68107 and 68108	INT - completely unmineralized Carb 2b, wk skeletal			
68110	EC08-003	22.90	6	Glim - py (40 - 60 %)	INT - mineralized glimmerite	22.50	24.24	Glim with thick (up to 10cm) zones of semi-mass py cut by mafic-poor, cg, w phl. Carb. The amount of py is very unusual. Py Glim 22.5-22.95, 24.0-24.24 Pieces:@ 22.9 (68110) - py Glim, @23.35 (68111) - Carb
68111	EC08-003	23.35	9	Carb - pk-cr, pych?-phl				
68112	EC08-003	47.00	6	Carb - med gy, blk f.g. spekling throughout, pych? (some r-br tint)	INT - mineralized 1b	46.80	48.40	46.8-47.6 f.g. mafic rich Carb, med br-grey. 47.6-48.4 c.g. streaky, phl Carb - quite possibly Carb 2. Pieces:@47.0 (68112) 47.0 fg, @ 47.9 (68113) c.g.
68113	EC08-003	47.90	6	Carb - same litho as 68112 but c.g.	INT - mineralized 1b			
68114	EC08-003	64.85	10	Silicocarb - f.g-m.g, cc (few), mag (abnt)	INT - high Nb, low Ta	64.35	66.27	f.g. - m.g., v mag rich, cc poor, Silicocarbonatite mag f.g. and super abnt, +50% Piece:@64.85 (68114)
68115	EC08-003	67.10	7	Silicocarb - dk gy, mag (abnt), py, pych? (r-br specks)	INT - high Nb, low Ta	66.27	67.20	SA above v mag-rich Silicocarbonatite, possible Carb 1. More c.g. and more cc. More lt coloured (med dk gy vs. dk gy) Rock above 64.35 is c.g., non-skeletal, Carb 2. Rock below 67.2 looks like m.g., somewhat mafic rich Carb 1. Piece:@ 67.1 (68115)
68116	EC08-003	72.45	11	Carb 2 - med gy, skeletal, phl-mag-ap-pych, py (minor)	INT - high Nb, low Ta	71.18	73.18	F.g., mafic-rich, Carb 1 cut by m.g. sparsely mag-phyric Carb 2, wk skeletal texture Carb 2 - 71.85-72.05, 72.25-72.7 Pieces:@72.45 (68116) - Carb 2, @73.05 (68117) - Carb 1
68117	EC08-003	73.05	10	Carb 1 - v f.g., r-br min, pych? (dk gy)	INT - high Nb, low Ta			
68118	EC08-003	90.40	15	Carb 2 - mafic (abnt), mag (pheno), pk-gy, py, gr prismatic min???	INT - high Nb, low Ta, unknown gr prismatic min	89.52	90.60	Mafic rich, c.g., Carb 2. F.g., ap, mag, phenos, minor py. Subhedral dk gy-gr prisms-what are these?-clb. Rare 5mm Carb 4 vnlets. Mafic rich patch. Piece:@90.3-90.45 (68118)
68119	EC08-003	106.75	13	Carb 2 - c.g., clb? (gy-gr prismatic min)	INT - described as prominent 'clb'	105.47	107.21	"Prominent clb". Rock is a c.g., wk to mod foliated Carb 2. Slight variationsin mafic min abundance. M.g. - v c.g. pheno mag, common gy-gr prismalic min, minor py and common "clb", dk br min, equant, not small, dirty y when cut [?? Not sure??] by saw. Prominent. What is this min? Pieces:@106.75 (68119), @109.75 (68120)
68120	EC08-003	109.75	9	Carb 2 - same litho as 68119	INT - described as prominent 'clb'			
68121	EC08-003	112.80	9	Carb - dk gy	INT - wkly mineralized Carb 1b	110.00	123.00	110.00-+/-112.5 m.g. foliation Carb 2 -117.25 f.g., mafic rich Carb 1 to Silico with OC Glim near base -123.00 vv f.g., lt gy Carb vnlets cut lt tan, suc Carb 3 real ctc. Pieces: @112.8 (fg)(68121), @119.85 (vned Carb 3)(68122)
68122	EC08-003	119.85	6	Carb 3 - vns, lots of vugs	INT - wkly mineralized Carb 1b			
68123	EC08-003	170.15	11	Carb 2 - lt gy, mag-phl-py±clb	INT - high Nb, very low Ta	167.65	180.10	Fairly homo interval. Patchy-diss mod mafic abundance Carb 2. Phenos of phl-mag, lesser from grained py and dk br clb-not abnt. Occasional gy-gr min. Min contains occasional swirly patches of m.g.-c.g. Silicocarbonatite. (171.80-172.40, 173.45-173.7) Pieces: @170.15 (68123), @176.50 (68124), @179.00 (68125)
68124	EC08-003	176.50	13	Carb 2 - similar litho to 68123 but more abnt clb	INT - high Nb, very low Ta			
68125	EC08-003	179.00	8	Carb 2 - same litho as 68123 but more pk	INT - high Nb, very low Ta			
68126	EC08-003	188.75	13	Carb - med gy, mag-phl-ap-clb-py	INT - high Nb, high Ta, lots of clb	188.40	189.20	Mod. Mafic-rich, c.g. Carb 2. No skeletal. Generally the same mineralogy as above. Ex. Less phl, more mag phenos, more ap, much more "clb". Ap as clear-gr clusters, clb common, tends to cluster near patches of mag phenos. mag-phl-ap-clb-py Pieces: @188.75 (68126), @189.05 (68127)
68127	EC08-003	189.05	7	Carb - med gy, mag-phl-ap-clb-py	INT - high Nb, high Ta, lots of clb			
68128	EC08-006	103.45	10	Carb 4 - v f.g. dyke, med-dk y-gy ±py	INT - returned 0.98% REE+Y, second highest in dataset	103.11	104.21	Swirled, v v f.g. dk olive gr Carb 4 dyke. The lower half (below 103.55) is brec with small, fract. Lt. Coloured carb matrix. Dyke cuts Carb 3 suc with common hem (after mag?) small phenos. Piece: @103.45 (68128), @104.05 (68129), @104.9 (Carb 3 with phenos)(68130)
68129	EC08-006	104.05	10	Carb 4 - v f.g. dyke, med-dk y-gy ±py	INT - returned 0.98% REE+Y, second highest in dataset			
68130	EC08-006	104.90	11	Carb 3 - y-gy, zoning of equant blk-r grains, unit cut by Carb 4 dykes (68128, 68129)	INT -adjacent to high REE. Not sure why A.K. Selected			
68131	EC08-007	70.65	7	Carb 2 - skeletal, mafic rich, pych? (abnt dk r-br blebs)	WRONG INTERVAL - INTENDED THE PRIOR 4 M	70.45	78.10	This interval is streaky, rather mafic-poor, non skeletal, Carb 2 dyked and locally altered by v v f.g. med gr-br late carb (Carb 4?). Carb 2 bx and infilled by v v f.g. Carb 4 locally. 70.45-70.75 mafic-rich, skeletal Carb 2. 70.75-70.95 S4 dyke. 70.95-73.05 mafic-poor Carb 2, Glim and bx in lowest 45cm. 73.05-75.30 Complex of Carb 4 dykes and bx and slightly altered Carb 2. Brec infilled with Carb 4 40% Carb 4 material overall.-78.10 mod to wk mafic min content py-phl only mag phyric locally. One spot has pale gr 1-2mm "blobs" associated with mag phenos (75.95) Pieces: @70.65 (mafic rich skeletal Carb 2), @74.15 (gr altered Carb 2), @75.1 (S4), @77.55 (boring, mafic-poor Carb 2), @76.00 (gr blob Carb 2 with mag)
68132	EC08-007	74.15	14	Carb 2 - gr-y alt, fl (blebs pervasive)	WRONG INTERVAL - INTENDED THE PRIOR 4 M			
68133	EC08-007	75.10	12	Carb 4 - v f.g., gr-gy dyke	WRONG INTERVAL - INTENDED THE PRIOR 4 M			
68134	EC08-007	77.55	6	Carb 2 - mafic (few), streaky nature concentrating some mafics, unknown blk specs, cr min	WRONG INTERVAL - INTENDED THE PRIOR 4 M			
68135	EC08-007	76.00	12	Carb 2 - mag, po, unknown gr blobby min (lt to dk)	WRONG INTERVAL - INTENDED THE PRIOR 4 M			
68136	EC08-013	104.20	13	Carb 4 - v f.g. dyke, olive gr, med gy / Carb 3 - minor frags	INT - returned 0.95% REE+Y, 4th highest in dataset	102.83	104.72	v f.g., completely mass med-dk olive gr Carb w occasional frags of f.g. Carb 3. Large mass of Carb 4. Next interval the same with much more Carb 3 frags included. Piece: @104.2 (68136)
68137	EC08-013	139.70	10	Carb 4 - v f.g. med dk gr-gy dyke / Carb 3? - abnt small clast incl. (more than 68136)	INT - returned 0.97% REE+Y, 3rd highest in dataset	138.94	140.07	interval of dk gr, v f.g. Carb with abnt small included Carb frags. Surrounding streaky Carb 3. Piece: @139.70 (68137)
68138	EC08-014	24.30	8	Carb - fl (p interbedded), unknown y min	Unidentified y min	24.24	24.31	Dk p fl interbnded with Carb and y min. Short segment in brec v f.g. olive Carb and also bnded fl-y min. Piece: @24.30 (68138), @26.15 (68139)
68139	EC08-014	26.15	6	Carb - fl (p interbedded), unknown y min	Unidentified y min			
68140	EC08-014	33.40	11.5	Carb 4 - v f.g., dk olive gr med gy dyke, py (minor), fl (minor), lt speckling of f.g. blk min	INT - returned 0.68% REE+Y within ~10 m zone of 0.57% REE+Y	32.79	34.05	V v f.g. dk olive gr Carb with numerous inclusions. -frags of lt tan Carb locally resembles brec. Intervals below contain more and longer frags-inclusions. Carb 4 with abnt Carb 3 frags? Piece (piece selected is relatively inclusion-free): @33.40 (68140)
68141	EC08-014	163.50	14	Silicocarb - v v c.g. mag, Carb and fl matrix	INT - very low Ta, mod Nb, unusual litho	162.81	163.85	V v f.g. mag silicocarbonatite horizon [?] with matrix of carb and p fl in Carb 3. Very unusual. Silico ends at 163.85 but occasional course patches of p fl abnt at +/- 169.60. Piece: @163.50 (68141)
68142	EC08-014	177.95	10	Carb 3 - f.g. olive gr, mafic rich, clb (abnt), pych? (r-blk min), cc? (patchy clear w xtls)	INT - mod Ta zone	175.70	182.37	High Ta zone. Swirly textured mafic-rich, f.g. gr-ish Carb 3. Mafics increase in abundance below 172.5. Below 182.37 rock is significantly more mafic-poor and even textured Carb 3. Piece: @177.95 (68142), @181.75 (68143)
68143	EC08-014	181.75	8	Carb 3 - simlar litho to 68142, but with more abnt pych? and lack of clear w xlts	INT - mod Ta zone			

Values have been corrected for driller depth error (EC08-016-020)

Sample	Hole	Depth (m)	~Thin Section Length (cm)	Sample Decription	Reason For Selection	Interval Description		Remarks
						From	To	
68144	EC08-015	201.52	7	Fl - streaks of y-gr Carb 3 / Carb 3 - v f.g speckles blocks	Mass fl section in hole EC08-015	182.27	183.52	med to well streaky foliated (+/- 90°+ca), med to dk gr suc Carb 3. Mafics f.g., a blk equant min, a tan rhombrohedral min (Knox hadn't seen before) and minor py. Tan min most abnt, mafics overall abnt. Minor p fl streaks throughout. Well developed, streaky foliation distinctive compared with surrounding intervals. Pieces: @201.52 (68144){Carb and fl), @182.50(68145)
68145	EC08-015	182.50	10	Carb 3 - abnt unknown tan-br min, fl (streaks), py (minor), pych? (round r-blk)	Unidentified tan rhombohedral min, 1.8% Nb with 38 ppm Ta			
68146	EC08-015	202.75	9	Silicocarb - mag pheno, py (equant), fl, pych? (round blebs resembling pych are common)	Last sample in hole, new litho + highest overall Nb-Ta-U assay	202.57	203.30	This interval is mostly v c.g., anh mag Silico. 202.21-202.36 swirly bnded p fl. 202.36-202.46 v c.g. mag Silico. 202.46-202.55 Glim frag with cc vnlets. 202.55-203.1 v c.g. mag Silico. 203.1-203.16 f.g., suc, dk gr Carb 3. 203.16-203.25 60% large fl patches in Carb 3. 203.25-203.30 f.g., suc, dk gr Carb 3. The v c.g. mag Silico consists of anh large mag and lesser fl phenos (!) with a finer, euh py, in a v f.g. Carb 3 matrix. Mag 65%. Associated with the mag are much finer dk equant mins -pych? Piece: @202.75(68146)
68147	EC08-016	103.00		Carb 3 - y olive-gr, py-fl, minor blk spots, unknown tan mineral	INT - Nb>3000, Ta<7.5, U<7.5, unknown tan min	104.19	111.62	Carb 1. Swirled to wkly streaky foliated lt to dk gr to cr Carb 3. Interval below is dker coloured as is one above (not as marked). Mafic f.g., py-tan equant min. [??word??] interval contains fine, diffuse fl-rich blebs. Occasional p fl filled fract and voids with py. Pieces: @104.65(68147), @109.45(68148), @110.90(68149)
68148	EC08-016	107.73	9	Carb - lt to med gy, mafic poor, py (minor), unknown tan min	INT - Nb>3000, Ta<7.5, U<7.5, unknown tan min			
68149	EC08-016	109.15	9	Carb - med-dk gy, py (minor), fl (minor), mafic poor, uknown tan min	INT - Nb>3000, Ta<7.5, U<7.5, unknown tan min			
68150	EC08-019	117.30	5	Carb 4? - v f.g., dk-gy-gr, hem? (red streaks)	Want confirmation on r streaks, different litho			v f.g. gy-gr. Carb 4? Piece: @119.18(68150)
68151	EC08-019	193.36	15 (193.21 - 193.36)	Silicocarb - mag (abnt c.g.), 3 mins unknown/questioned (1. br-y 10% pych?, 2. gr-gy, 3. r-br pych?)	Expected 10% pych and great assay. It was average only	196.46	196.60	Swirl of Carb 2 Silicocarbonatite. C.g. mag-br pych and the gr-gy unidentified min. The br min is 10% miner py. Piece: 196.30-196.45 (68151)
68152	EC08-021	3.8	10	Carb 3 - gy-gr, py-fl, pych? (f.g. blk min)	INT - high Nb, low Ta	2.25	12.46	F.g., suc Carb. Blotchy in shades of gr, mostly dk gr abnt, diss py, fine fl blebs and fine equant blk min. Irregular dispersed f.g. - m.g. Glim frags. Pieces: @3.8(68152), @7.45(68153), @11.05(68154)
68153	EC08-021	7.45	10	Carb 3 - gy-gr, py-fl, pych? (f.g. blk min)	INT - high Nb, low Ta, contrast with 68156?			
68154	EC08-021	11.05	8.5	Carb 3 - gy-gr, py-fl, pych? (f.g. blk min)	INT - high Nb, low Ta			
68155	EC08-021	13.15	9.5	Carb 3 - very similar to 68152, more y-gr, py-fl (clasts and blotches), pych? (f.g. blk min)	INT - high Nb, low Ta	12.45	18.10	Swirly textured Carb 3, colour mottled in shades of gr, mostly dk gr. F, Carb frags common as are diss fl rich blebs. Py and a v f.g. equant blk mafic min. Some phl in lt coloured sections. Where accidental frags are abnt rock has pseudo bx texture. Pieces: @13.95(68155), 16.35(68156), @17.65(68157)
68156	EC08-021	16.35	10	Carb 3 - gy-gr, brec, py-fl (clasts and blotches), pych? (f.g. blk min), cr carb is major clast	INT - high Nb, low Ta, contrast 6.71 - 7.71 m with 15.53 - 18.10 m			
68157	EC08-021	17.65	8.5	Carb 3 - gy-gr, brecc, py-fl (more blotchy than clasts), pych? (f.g. blk min more than 68156), blotchy unknonw br-ish min	INT - high Nb, low Ta, contrast 6.71 - 7.71 m with 15.53 - 18.10 m			
68158	EC08-021	66.85	9	Carb 3 - gy-gr, py-fl, unknown cr-br min speckled throughout	Look at Nb zones 63.92 - 73.51 and 78.43 - 92.85 m, relationship between Nb, fl and cr-br min	65.35	92.85	The fl-py-cr Carb zones are obviously open space filling. These are very low in Nb-Ta and show no Carb geochemical affinity. Late. The surrounding Carb is swirly-mottled, mainly dk gr Carb 3, locally with more lt coloured frags (xenoliths?) within. Mostly Fl-Py-Carb infill. 67.70-70.00, 73.60-78.40. The Carb contains diss py and a fine, tan, equant min, along with Fl-rich blebs and cr carb xenos. What is tan min?? Pieces: @66.85 (68158), @71.75(68159), @79.95(68160), @82.30(68161)
68159	EC08-021	71.75	8	Carb 3 - gy-gr, py-fl, unknown cr-br min speckled throughout (less than 68158)	Look at Nb zones 63.92 - 73.51 and 78.43 - 92.85 m, relationship between Nb, fl and cr-br min			
68160	EC08-021	79.95	11	Carb 3 - gy-gr, abnt unknown tan-r-br min, minor unknown cr-br min, py-fl-phl	Look at Nb zones 63.92 - 73.51 and 78.43 - 92.85 m, relationship between Nb, fl and cr-br min			
68161	EC08-021	82.30	8	Carb 3 - med dk-gy-gr, unknown cr-br min, r-br min, py-fl, minor blk min	Look at Nb zones 63.92 - 73.51 and 78.43 - 92.85 m, relationship between Nb, fl and cr-br min			
68162	EC08-021	88.35		Carb 3 - gy-gr, py-fl, unknown cr-br min speckled throughout	Look at Nb zones 63.92 - 73.51 and 78.43 - 92.85 m, relationship between Nb, fl and cr-br min	92.85	116.70	92.85-100.80 75% Fl-Py-Carb open space filling with interbnded lt gy Carb 3, mafic-poor carb. To 105.50 mostly lt gy Carb with narrow zones of py-fl-Carb open space fill vnlets and Bx matrix. The lt gy Carb is mottle-textured with diss py, lesser diss fl, the tan, equant (often square) min, rare thin streaks of phl and diss hem? The fine, often square tan mins are sometimes almost w and may be crystal aggregates. Knox would guess they carry Nb-Ta. All the carb is Carb 3, f.g. to v f.g. and suc textured. Pieces: @88.35(68162), @102.10(68163), @104.05(68164)
68163	EC08-021	102.1		Carb - mottled looking gr-y, py-fl-phl, unknown minor blk min	INT - abnt py-fl infill with abnt Nb			
68164	EC08-021	104.05	6.5	Carb 3 - med to lt gy, py-fl-minor mafics, doesn't look overly special	INT - abnt py-fl infill with abnt Nb			
68165	EC08-021	113.35	10	Carb 3 - py-fl, f.g. blk dk br min (pych?), tan-cr min (not overly abnt)	INT - high Nb, high Ta, unknown tan min	111.13	111.45	Swirly mottled, med gy gr, f.g. suc-textured Carb 3. Interval contains +/- 15% p fl-carb fine vug infills. The Carb contains 3 mafic (non-carb) mins, all f.g. py- a dk br equant min (pych?) -cr-tan equant square min. The pych? is equant but anh with slightly clumpy distribution. Mottling defined by colour variations. No clasts xenoliths. Piece: @113.35 (68165)
68166	EC08-021	177.90	10.5	Carb 2 - pk, mafic rich, mag-pych(minor), unknown ovoid gr glassy min	Unknown ovoid gr glassy min	176.00	182.25	176.00-177.00 Bnded, c.g. Carb 2 mafics arranged in 1-4mm bnds, separated by cr Carb. Bnding +/- 90°+ca. 177.00-182.25 Same, with common patches of swirly Silicocarbonatite. Mag phenos and f.g., ap and f.g.-m.g. br pych. Locally present are ovoid, internally fractured med gr glassy min. Pheno ap? Aegrine? 181.00-182.25 Long patches of shiny skeletal texture. Pieces: @177.9 (68166), @181.10(68167)
68167	EC08-021	181.10	9.5	Carb 2 - similar to 68166 but less mag, skeletal, r blotches	Unknown ovoid gr glassy min			
68168	EC08-021	196.00	8.5	Silicocarb - dk gy, mag-pych, ± dk gr min	INT - high Nb, high Ta, 1450 cps	195.90	196.10	(Carb 2) Layer of Silicocarbonatite. Pheno mag and dk gy-gr min, finer phl-pych-py. Abnt f.g. glassy ap. This thin Silico is mineralogically bnded, poorer in mag at top and bottom (richer in phl and the gr-gr min). Silico is cut by 2cm pk mafic poor Carb vn. The Carb below the silico is m.g. and bnded. Alone is c.g. w mag phenos and much more mass. Cycle ctc? Piece: 196.00(68168))
68169	EC08-021	200.15	9	Carb 2 - pk to dk pk-r, br to dk-r min (pych/clb?), lt gr patchy min, nil mag	INT - well mineralized Nb-Ta, pych/clb??	199.60	204.80	2 Carb cycles (Carb 2) 196.1-201.75,-204.8. Both start out mafic poor (top one also bnded). Downwards in each cycle the grain size coarsens and mafics become more abnt. Both have Basalt Silico (201.35-201.75, 204.20-204.80) One skeletal patch, 202.35-202.75. Mag (pheno)-gy-gr min-py-pych and f.g. ap. The gy-gr min often looks like crystal aggregates-anh. Pieces: @200.15(68169), @203.15(68170), @204.40 silico, (68171)
68170	EC08-021	203.15	8.5	Carb - pk to dk r, streaky-bnded, mafic rich, mag phenos, gr min abnt, clb/pych?	INT - well mineralized Nb-Ta, pych/clb??			
68171	EC08-021	204.40	9.5	Silicocarb - pk, mag rich, clb/pych?, unusual br streaks??, gr min common	INT - well mineralized Nb-Ta, pych/clb??			
68172	EC08-021	126.50		Carb 2 - c.g., phl-ap-py-mag, local Carb 1 present	?	125.00	129.00	Somewhat swirly textured c.g. phl-ap-py-mag Carb 2 mafic mod-abnt, in diffuse bnds and swirly. Not well mineralogy, locally Carb 1 pk-ish cast. Piece: @126.50 (68172)
68173	EC08-026	175.15	11	Carb - cr, mafic bnds, unknown tan-cr equant min confined to bnds, phl-ap-py-mag	INT - very low Ta, mod Nb	174.25	175.32	This sample is in a much larger interval (at least 170-182) of mod bnded Carb 2. Mafic rich bnds 0.5-4cm alternate with essentially mafic free carb (cc?) Phl-py-ap-mag. And a lt cr to tan to flesh equant f.g. min often with sharp corners. (Interesting mineralogy) Carries the Nb? Pychl? Entirely confined to mafic bands/streaks. Bnding 75-90°+ca. Piece: @175.15(68173)
68174	EC08-026	100.35	10	Carb 2 - med gy, br min reminiscent of pych, mag-py-unknown gr min	INT - appears at typically mineralized Carb 2 but no Ta or Nb as mineralogy suggests	95.93	111.50	C.g., mag phyric Carb 2. All textures, bnded, clumpy mafics, some skeletal texture, some Silicocarbonatitemafics med to locally abnt. Mag phenos-gy-gr min phenos-ap-minor py, less phl. Pych present but nowhere near common, also small grains. This is a typical mineralized Carb 2 but pych conspiciously absent. Strange, good looking section without much pych. Locally strong RA and anomalous RA throughout. Why no pych??? Pieces: @100.35(68174), @104.30 (68175){mineralized), @109.90(68176)
68175	EC08-026	104.30	9	Silicocarb - pych, mag (abnt phenos), phl, gr patchy min	INT - mineralized interval but no mineralization surrouding as mineralogy would suggest			
68176	EC08-026	109.90		Carb 2 - lt to med gy, mag (phenos abnt), dk gr pheno xts abnt, pych	INT - very low Ta, mod Nb			

Values have been corrected for driller depth error (EC08-016-020)

Sample	Hole	Depth (m)	~Thin Section Length (cm)	Sample Decription	Reason For Selection	Interval Description		
						From	To	Remarks
68177	EC08-026	134.65	10	Carb 2 - med gy, phl-py-ap-mag, pych (equant grains), intrudes cr Carb 1	INT - mineralized with lots of Glim in it	132.36	145.39	This interval consists of c.g. phl-py-ap-mag carb containing +/-30% blk Glim frags. The Glim is as large mass bodies riddled with f.g.cc veinsor smaller elongate pieces parallel to the min bnding. The lowest large piece ends @140.80. Bnding 80-90°+CA. Carb mafics f.g., largest is phl. Pych possible as fine blk square crystals or in one piece (134.65) as br equant grains. I couldn't see any in the Glim itself. Definately Carb 2 including Glim at top. Below 141 only Carb 1? Pieces: @134.65(68177), @140.10(68178), @142.95(68179)
68178	EC08-026	140.10	14	Carb - dk gy, mafic rich, py-phl, pych? (occasionaly) / Glim - frags common (< 1 cm)	INT - mineralized with lots of Glim in it			
68179	EC08-026	142.95	8.5	Carb 1-2 - cr, mafic streaks, phl, minor py, blk flecks (pych?), ap (minor streaks)	INT - mineralized with lots of Glim in it			
68180	EC08-006	64.30	9	Carb 2 - dk gy, borderline silicocarb, mag (abnt), unknown pale y-gr min, clb/pych (abnt)	INT - differing Nb-Ta ratios	63.40	76.50	Carb 2 mineralized with occasional Glim frags. Lots of v f.g. mag silico with common clb/pych. These v c.g. silicos are long and v cc poor. Also abnt. V c.g. skeletal texture. Overall interval is mafic rich. A very good looking interval ag-oviod gr min-ap-py. Clb is abnt in some of the silicos. Pieces: @64.30(68180), @66.90(68181), @72.50(68182), @74.15(68183)
68181	EC08-006	66.90	8	Silicocarb / Carb 2 - mag pheno, dk gr min, clb-pych (abnt) / Carb 2 - lt gy, mag (streaky), gr min, clb-pych (minor)	INT - differing Nb-Ta ratios			
68182	EC08-006	72.50	10	Carb 2 - patchy silicocarb, mag rich, py-clb/pych (r rims on some grains), two unknown gr mins (1. dk 'forrest' gr, 2. more lt 'grass' gr)	INT - differing Nb-Ta ratios			
68183	EC08-006	74.15	12.5	Carb 2 - same as 68182 but far less clb-pych	INT - differing Nb-Ta ratios			
68184	EC08-009	119.35	9	Carb 2 - lt gy, homo, mag (abnt), unknown ovoid lt 'grass' gr min, clb (abnt), py (minor)	INT - clb is present but does not run	107.05	140.90	Skeletal Carb 2 with mafic poor zones. Although clb is abnt in mag pheno rich patches, maybe not enough to overcome mafic poor sections. Ovoid to amorphouus gr min common in mag rich sections. Pieces: @119.35(68184), @125.60(68185), @129.85(68186), @130.75(68187), 136.30(68188)
68185	EC08-009	125.60	13	Carb - cr, mass, patches of mag-unknown forrest gr min, py, clb (abnt)	INT - clb is present but does not run			
68186	EC08-009	129.85	10	Carb 2 - lt gr (alt), mag (minor, alt to hem?), py (minor), clb/pych not apparent but may be the f.g. blk specks present	INT - clb is present but does not run			
68187	EC08-009	130.75	7	Carb - pk-gy, mag (c.g.), clb (c.g.), unknown c.g. med gr min, mag-clb-gr min are not huge % of total	INT - clb is present but does not run			
68188	EC08-009	136.30	9.5	Carb - lt pk, mafic mod, phl-mag, py(minor), ap(streaks), clb (present but more f.g. than previous samples in interval)	INT - clb is present but does not run			
68189	EC08-025	17.40	12	Carb 2 - lt gr-gy (alt), mag (phenos), py (abnt), pych? (f.g. br-blk	INT - zone of highest Ta-Nb			-
68190	EC08-025	21.30		Carb 2 - dk pk, large mafic content, mag (abnt), pych? (dk r xts)	INT - zone of highest Ta-Nb			-
68191	EC08-025	22.40	8	Carb 2 - med gy, mag (c.g.), py (minor), pych? (f.g. blk specks)	INT - zone of highest Ta-Nb			-
68192	EC08-025	47.05	6.5	Carb 2 - gr, mafic abnt, ap, mag (phenos), py (minor), ± pych/clb	INT - zone of highest Ta-Nb			-
68193	EC08-025	48.00	8.5	Carb - lt gy-gr (ap), mod mafics, some bnding, pych? (speckled blk min), nil py-mag	INT - zone of highest Ta-Nb			-
68194	EC08-025	45.20	8	Carb - med gy-gr, mafic abnt blotches, mag (phenos), py (minor), fl (minor), pych? (blk min), pseudo breccia appearance	INT - zone of highest Ta-Nb			-
68195	EC08-016	129.28		Carb 3 - med gr-gy, py (minor), fl (blotchy patches), pych (diss; appears in two phases, one lt and one dk)	?			-
68196	EC08-019	151.53	12	Silicocarb - med gy-bl tinge, mag (phenos), py (equant), phl (patches), unknown gr min	Differing Nb-Ta content in texturally similar sequence	145.67	168.80	This interval is a long section of Carb 2. The upper part (150.00-171.30, uncorrected) is relatively Nb, Ta poor. It has typical carb 2 textures including skeletal and silico but is poor in pych. Below 171.30 (uncorrected) the same textures are present, just there is more pych. In both sub intervals the Silico mineralogy is mag-unidentified dk gy-gr min (sometimes glass gr)-py-+/-pych. C.g. phl appears in min streaks outside of silico patches. The Silicocarbonatite patches are 30-50cm and most often appear at the ctc between bnded, relatively mafic-poor carb (below) and more mass carb above which is generally mafic-richer, with the mafics in patches and streaks. Thus the silico could represent cumulate cycles bases, each representing a seperate magma pulse. Many pieces taken, hopefully to illuminate why there is such a difference in Nb-Ta content in such a texturally similar sequence. The core pieces taken are each from mafic-rich sections of the core, and are not representative of the interval as a whole. Pieces: @153.95 (68196), @155.40(68197), @157.4(68198), @162.45(68199), @167.15(68200), @168.70(68201), @170.95(68202), @171.50(68203), @173.55(68204), @174.40(68205), @175.80(68206), @178.10(68207)
68197	EC08-019	152.95	12	Carb 2 - med dk-gy, mag (phenos), py, unknown gr min, unknown r min (hem? - don't think so), can describe in way more detail	Differing Nb-Ta content in texturally similar sequence			
68198	EC08-019	159.89	12	Carb 2 - med gy, streaky, bnded in pk mafic free Carb 1, mag-py-pych?, unknown br streaky min	Differing Nb-Ta content in texturally similar sequence			
68199	EC08-019	154.92	12.5	Carb 2 - lt gy, minor skeletal, mag (phenos), abnt dk gr and lt gr unknown min, clb (minor), py (minor)	Differing Nb-Ta content in texturally similar sequence			
68200	EC08-019	164.52	9.5	Carb - med gy-pk, mag (phenos), py (minor), unknown gr min, pych? with red halos (alt?)	Differing Nb-Ta content in texturally similar sequence			
68201	EC08-019	166.04	6.5	Carb - lt gy-pk, streaky, mag, grass-gr unknown min, py (minor), pych? (diss f.g. blk)	Differing Nb-Ta content in texturally similar sequence			
68202	EC08-019	168.26	12	Carb 2 - med gy, mod mafics, lt to 'forrest' gr unknown min, red alt min?, py (minor), clb/pych? (minor br-tan)	Differing Nb-Ta content in texturally similar sequence			
68203	EC08-019	168.80	8	Carb 2 - very similar to 68202, marginally smaller grain size	Differing Nb-Ta content in texturally similar sequence			
68204	EC08-019	170.82	8	Carb 2 - gy-pk, pych (abunt), unknown gr min, mag-phl, pervasive unknown r min	Differing Nb-Ta content in texturally similar sequence			
68205	EC08-019	171.65	9	Carb 2 - med gy, streaky, mag (abnt), pych, lt gr unknown min, py (minor equant)	Differing Nb-Ta content in texturally similar sequence			
68206	EC08-019	173.03	8.5	Carb 2 - same as 68206 but with unknown dk gr mineral as well	Differing Nb-Ta content in texturally similar sequence			
68207	EC08-019	175.29	9	Carb - med gy, c.g. mafics, unknown dk gr min, mag, pych (diss, much f.g. than previous samples)	Differing Nb-Ta content in texturally similar sequence			

APPENDIX 15B: LIST OF SAMPLES COLLECTED FOR THIN SECTION WORK (PROSPECTING ROCK)

See Appendix 4 for locations

Sample	Year Sampled	Waypoint
AK3A	2008	AK3A
42801	2008	AK010
42803	2008	AK015A
42807	2008	AK029
42808	2008	AK033
42812A	2008	-
42812B	2008	-
42814	2008	AH002
42816	2008	AH004
42817	2008	AH008
42818	2008	AH023
42819	2008	AH024
42820	2008	AK25
42829	2008	TM017
42852	2008	RD08-003
42855	2008	RD007
42859	2008	TM038
47728	2008	TM048
47729	2008	TM052
68005	2008	TM055
68007	2008	MG08-009
70001	2009	
70002	2009	-
70003	2009	-
70005	2009	-
70007	2009	-
70010	2009	-

Sample	Year Sampled	Waypoint
70013	2009	
70026	2009	-
70027	2009	-
70028	2009	-
70029	2009	-
70054	2009	-
70059	2009	-
70071	2009	-
70073	2009	-
70075	2009	-
38702	2009	-
38714	2009	-
38721	2009	-
38724	2009	-
43004	2009	-
43009	2009	-
43010	2009	-
68010	2009	-
68015	2009	-
68020	2009	-
68023	2009	-
70017	2009	-
70025	2009	-
70046	2009	-
70047	2009	-
0914Apr03	2009	-
0914Apr09	2009	-